Supporting Information for Langmuir

Growth-Induced Wrinkles and Dotlike Patterns of a Swollen Fluoroalkylated Thin Film by the Reaction of Surface-Attached Polymethylhydrosiloxane

Thierry Thami,*[,1] Michel Ramonda,[2] Lynda Ferez,[1] Valérie Flaud,[3] Eddy Petit,[1] Didier Cot,[1] Bertrand Rebière,[3] Bruno Ameduri*[,3]

[1] *Institut Européen des Membranes, IEM, Université Montpellier, CNRS, ENSCM, Montpellier, France*

[2] *Centre de Technologie de Montpellier, CTM, Université Montpellier, Montpellier, France*

[3] *Institut Charles Gerhardt de Montpellier, ICGM, Université Montpellier, CNRS, ENSCM, Montpellier, France*

Corresponding Authors*

Thierry Thami – *Institut Européen des Membranes, IEM, Université Montpellier, CNRS, ENSCM, Montpellier, France 34095*

Email: thierry.thami@umontpellier.fr

Bruno Ameduri – *Institut Charles Gerhardt de Montpellier, ICGM, Université Montpellier, CNRS, ENSCM, Montpellier, France 34095*

Email: bruno.ameduri@enscm.fr

Table S1. R-PMHS thin films prepared by hydrosilylation grafting of alkenes with H-PMHS (thickness h_0 = 0.8 µm) at T = 65 °C on two distinct substrates: (A) Si wafer and (B) Silicone Med-4750. The sample nomenclature is based on the molar ratio of alkenes (x) = $[R_f]_0/([R_f]_0+[R_{hex}]_0)$, where $[R_f]_0$ and $[R_{hex}]_0$ stand for the concentrations of $C_6F_{13}CH_2CH=CH_2$ (Allyl-C_6F_{13} or 1*H*, 1*H*, 2*H*, 3*H*, 3*H*-tridecafluorononon-1-ene) at t = 0 and $C_3H_7CH_2CH=CH_2$ (1-Hexene) at t = 0, respectively, summarized by $(R_f)_x(R_{hex})_{1-x}$-PMHS with R_f = $CF_3(CF_2)_5(CH_2)_3$– and R_{hex} = $CH_3(CH_2)_5$–. The same condition was used for test reaction at room temperature for R = R_{hex} on (B) in acetonitrile.

Nomenclature R-PMHS (mol %)	Substrates	Solvents	1-Hexene (µL)	Allyl-C_6F_{13} (µL)
R_f	(A)	toluene	–	250
R_f	(A), (B)	cyclohexane	–	250
R_f	(A), (B)	acetonitrile	–	250
$(R_f)_{0.75}(R_{hex})_{0.25}$	(A), (B)	cyclohexane	62	291
$(R_f)_{0.50}(R_{hex})_{0.50}$	(A), (B)	cyclohexane	125	194
$(R_f)_{0.25}(R_{hex})_{0.75}$	(A), (B)	cyclohexane	186	97
R_{hex}	(A)	toluene	250	–
R_{hex}	(A), (B)	cyclohexane	250	–
R_{hex}	(A), (B)	acetonitrile	250	–

Table S2. IR absorption frequencies[a] of pristine H-PMHS (5% crosslinked) and R-PMHS thin films (R = H, R_{hex} and R_f) on Si wafer (A) in transmission mode. Ratio of extinction coefficient ($\varepsilon_y/\varepsilon_{2169}$) at most relevant bands (y) normalized to Si–H stretching band at 2169 cm^{-1} as external reference (See section 5 for more details). The alkyl side chains grafted onto the polysiloxane backbone have the formulae: R_f = $CF_3(CF_2)_5(CH_2)_3$- and R_{hex} = $CH_3(CH_2)_5$-.

Group frequency	Vibration type	IR peak position y in cm^{-1} ($\varepsilon_y/\varepsilon_{2169}$) in the films		
		H-PMHS	R_{hex}-PMHS	R_f-PMHS
$\nu(CH_3)$	Stretching vibration $SiCH_3$ and CH_3	2967	2958	2962
$\nu_{as}(CH_2)$	Stretching vibration CH_2		2924 (1.61)	2908 (0.17)
$\nu_s(CH_2)$	Stretching vibration CH_2		2857	2889
ν(Si–H)	Stretching vibration	2169 (1)		
$\delta(CH_2)$	Scissoring vibration		1466	
$\delta(CH_3)$	Bending vibration $SiCH_3$	1262	1257	
ν(C–F)	Stretching vibration CF_2 and CF_3			1240 (3.17), 1207, 1191,1144
ν(Si–O–Si)	Stretching vibration	1101 (1.35), 1055	1097 (1.57), 1022	1100 (1.57), 1025
δ(Si–H)	Scissoring vibration	890, 839		
$\delta(CH_3)$	Rocking vibration $SiCH_3$	769 (0.83)	800 (0.87), 775	795 (1.09)

[a] ν, stretching mode; as, asymmetric; s, symmetric; δ, bending mode, values of $\varepsilon_y/\varepsilon_{2169}$ in parentheses.

Table S3. X-ray Photoelectron Spectroscopy (XPS) analyses summarizing the surface of pristine H-PMHS polymer (R = H) and functionalized surfaces $(R_f)_x(R_{hex})_{1-x}$-PMHS with $R_f = CF_3(CF_2)_5(CH_2)_3$- and $R_{hex} = CH_3(CH_2)_5$-, on Si wafers (A) and silicone Med-4750 sheets (B).

Substrates	R-PMHS films		Element (atom %)				Composition[a]	Fit C1s (atom %)[b]		
			Si	C	O	F		$\%CF_2$	$\%CF_3$	CF_2/CF_3
(A)	R = H	Found	36.1	30.7	33.2		$SiO_{0.92}C_{0.85}$			
		Calculated	*33.6*	*31.9*	*34. 5*		*$SiO_{1.025}C_{0.95}$*			
(A)	R_{hex}	Found	17.0	66.8	16.2		$SiO_{1.0}C_{3.9}$			
		Calculated	*11.1*	*77.4*	*11.4*		*$SiO_{1.025}C_{6.95}$*			
(A)	$(R_f)_{0.25}(R_{hex})_{0.75}$	Found	14.4	61.3	13.9	10.4	$SiO_{1.025}C_{4.3}F_{0.7}$	2.5	0.4	5.8
		Calculated	*7.7*	*59.3*	*7.9*	*25.0*	*$SiO_{1.025}C_{7.7}F_{3.25}$*	*9.6*	*1.9*	*5.0*
(A)	$(R_f)_{0.5}(R_{hex})_{0.5}$	Found	13.9	51.1	14.2	20.8	$SiO_{1.0}C_{3.7}F_{1.5}$	5.6	0.9	6.2
		Calculated	*5.9*	*49.8*	*6.0*	*38.3*	*$SiO_{1.025}C_{8.45}F_{6.5}$*	*14.7*	*2.9*	*5.0*
(A)	$(R_f)_{0.75}(R_{hex})_{0.25}$	Found	11.2	43.6	11.6	33.7	$SiO_{1.0}C_{3.9}F_{3.0}$	9.6	2.1	4.5
		Calculated	*4.8*	*43.9*	*4.9*	*46.5*	*$SiO_{1.025}C_{9.2}F_{9.75}$*	*17.9*	*3.6*	*5.0*
(A)	R_f	Found	9.9	35.6	10.0	44.5	$SiO_{1.0}C_{3.6}F_{4.5}$	13.2	3.4	3.9
		Calculated	*4.0*	*39.8*	*4.1*	*52.1*	*$SiO_{1.025}C_{9.95}F_{13}$*	*20.0*	*4.0*	*5*
(B)	R = H	Found	36.2	33.0	30.8		$SiO_{0.85}C_{0.91}$			
(B)	R_f	Found	9.9	36.3	9.9	44.0	$SiO_{1.025}C_{3.7}F_{4.5}$			

[a]Calculated from the theoretical monomer compositions for 5% crosslinked H-PMHS $(SiCO)_{0.95}(SiO_{1.5})_{0.05}$ named as $SiO_{1.025}C_{0.95}$ (R = H) and for $(R_f)_x(R_{hex})_{1-x}$-PMHS summarized as $SiO_{1.025}C_{0.95}(C_9F_{13})_x(C_6)_{1-x}$ by assuming a total hydrosilylation reaction in 5% crosslinked H-PMHS.

[b]Percentage calculated from the total number of atoms N_{tot} : $\%CF_2 = 5x/N_{tot}$ and $\%CF_3 = x/N_{tot}$.

Table S4. Carbon components and binding energies (± 0.2 eV) in the C1s XPS spectra of H-PMHS (R = H) and functionalized $(R_f)_x(R_{hex})_{1-x}$-PMHS thin films (x = 0, 0.50 and 1). The alkyl chains have the molecular formulae R_f = $CF_3(CF_2)_5(CH_2)_3$- and R_{hex} = $CH_3(CH_2)_5$- where R is grafted onto the polysiloxane backbone.

R-PMHS films	Si–<u>C</u>	C–C	<u>C</u>F_2	<u>C</u>F_3
R = H	284.4	285.2		
R_{hex}	284.4	284.8		
$(R_f)_{0.5}(R_{hex})_{0.5}$	284.3	284.7	291.7	293.9
R_f	284.1	285.1	291.4	293.6

Table S5. Thickness of functionalized polymer R-PMHS thin films and Energy Dispersive X-ray spectroscopy (EDX) analysis at the surface with R_f = $CF_3(CF_2)_5(CH_2)_3$- and R_{hex} = $CH_3(CH_2)_5$-, on Si wafers (A) and silicone Med-4750 sheets (B) measured in a typical surface area of about 25 μm × 50 μm. Mean compositions and standard deviations from three measurements.

Substrate	R-PMHS thickness	Element (atom %)			
	(μm)	Si	C	O	F
R_{hex}-PMHS					
(A)	1.89	16.4 ± 0.5	70.9 ± 0.1	12.7 ± 0.4	
(B)	1.00	12.8 ± 0.4	74.3 ± 0.8	12.9 ± 0.4	
	*Calculated**	*11.1*	*77.5*	*11.4*	
R_f-PMHS					
(B)	0.95	8.2 ± 0.3	48.6 ± 0.4	8.2 ± 0.1	35.0 ± 0.8
	*Calculated**	*4.0*	*39.8*	*4.1*	*52.1*

*Calculated from the theoretical compositions for $(R_f)_x(R_{hex})_{1-x}$-PMHS, summarized as $SiO_{1.025}C_{0.95}(C_9F_{13})_x(C_6)_{1-x}$ with x = 1 and x = 0 for R_f and R_{hex} pure substituents, respectively, by assuming a total hydrosilylation reaction in 5% crosslinked H-PMHS (α = 0.95) of theoretical monomer composition $(SiCO)_{0.95}(SiO_{1.5})_{0.05}$ named as $SiO_{1.025}C_{0.95}$ (R = H).

Table S6. EDX analysis at the surface of dotlike pattern of polymer R_{hex}-PMHS (*h* = 1.89 µm) on Si wafers (A) in selected flat (1) or rough (2) scanned surface areas of about 0.25 µm × 0.25 µm (See white square frames 1 and 2 in Figure S17).

Analyzed region	Element (atom %)		
	Si	C	O
0.25 µm × 0.25 µm (Flat zone 1)	14.1 ± 0.9	74.5 ± 0.5	11.4 ± 1.3
0.25 µm × 0.25 µm (Peak zone 2)	14.3 ± 1.0	74.7 ± 0.3	11.0 ± 1.0
*Calculated**	*11.1*	*77.5*	*11.4*

*Calculated from the theoretical monomer composition R_{hex}-PMHS, summarized as $SiO_{1.025}C_{0.95}C_6$ by assuming a total hydrosilylation reaction in 5% crosslinked H-PMHS (α = 0.95) of theoretical composition $(SiCO)_{0.95}(SiO_{1.5})_{0.05}$ named as $SiO_{1.025}C_{0.95}$.

Table S7. Dispersive (*d*) and polar (*p*) components of liquids used for contact angle measurements. The total liquid surface tension is $\gamma_L = \gamma_L^d + \gamma_L^p$.

Liquid	γ_L (mN/m)	γ_L^d (mN/m)	γ_L^p (mN/m)
Water	72.8	21.8	51.0
Ethylene glycol	48.0	29.0	19.0
n-Hexadecane	27.5	27.5	0

Table S8. Total surface energy, dispersive and polar components of the "flat" functionalized R-PMHS films on Si wafer substrates (A)[a]

R-PMHS film	γ_S (mN/m)	γ_S^p (mN/m)	γ_S^d (mN/m)
R_{hex}	25.6	0.3	25.3
R_f	15.0	0.01	15.0

[a]Calculated from water contact angle, ethylene glycol contact angle and *n*-hexadecane contact angle (Figure 8) using the Owens and Wendt's method[S1] (Section 6 and Figure S18) where the surface energy of the solid is given by: $\gamma_S = \gamma_S^d + \gamma_S^p$. The R-function grafted onto the polysiloxane backbone has the molecular formulae: R_{hex} = $CH_3(CH_2)_5$- and R_f = $CF_3(CF_2)_5(CH_2)_3$-.

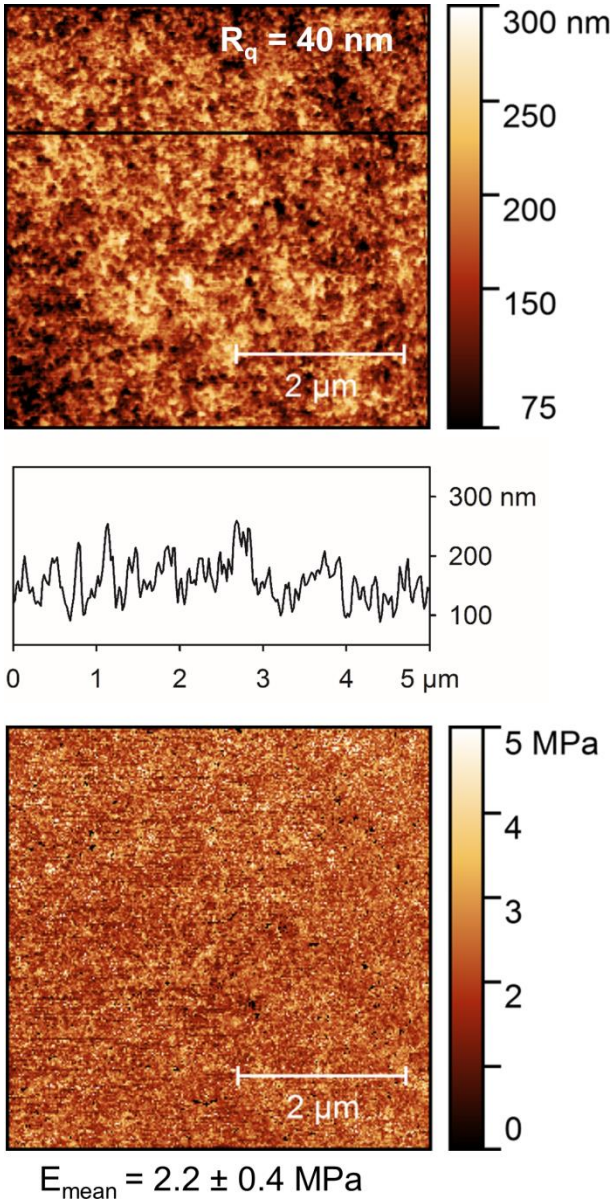

Figure S1. Representative maps of topography (top) and (bottom) elastic modulus calculated using the Johnson-Kendall-Roberts (JKR) model[S2] in PeakForce Quantitative Nanomechanical Mapping (PF-QNM) mode of pristine silicone Med-4750 substrate (bare sheet) (B). Profile section analysis according to the black line shown in height images. Elastic modulus E_{mean}: mean values of image.

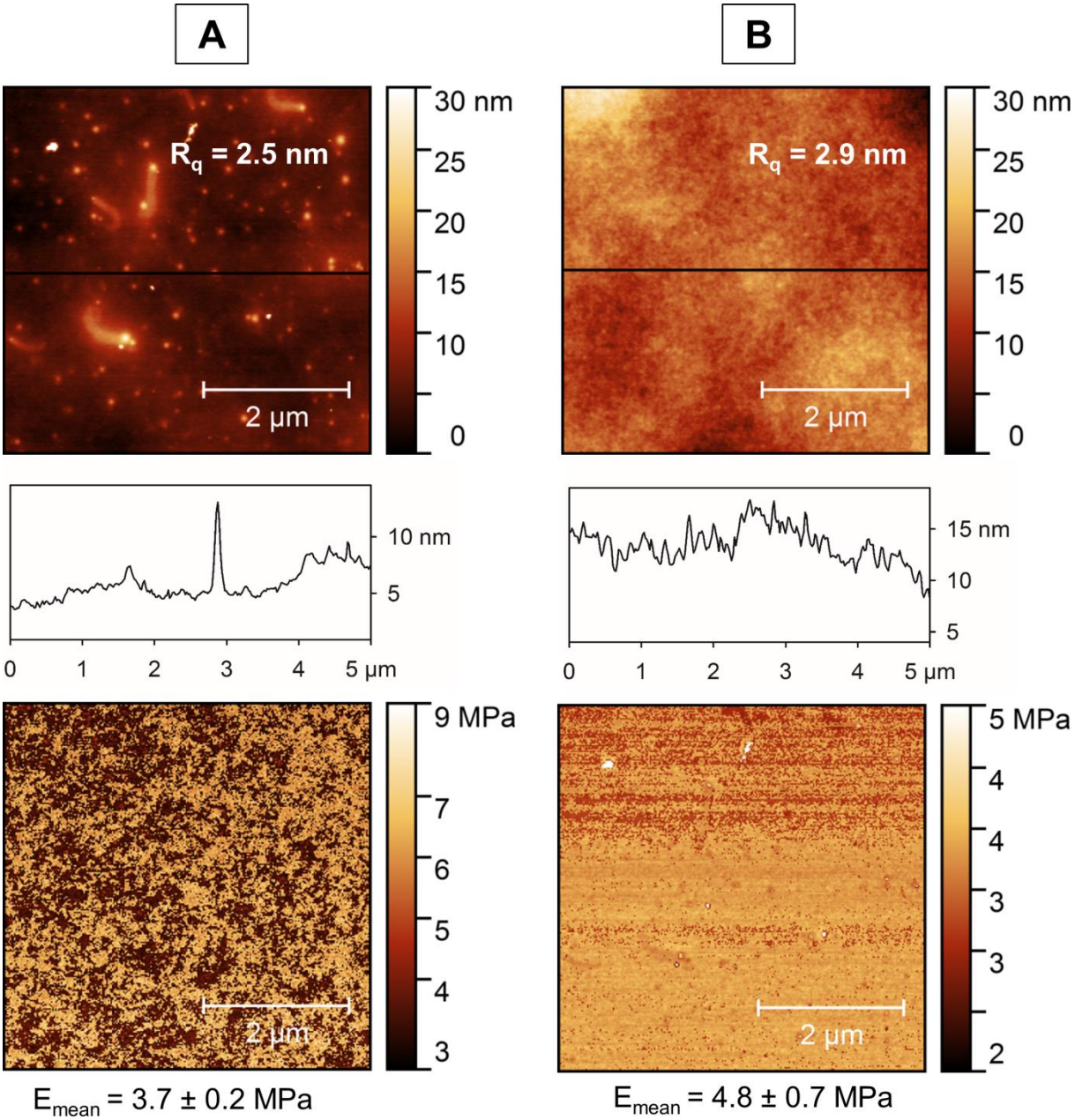

Figure S2. Representative maps of topography (top) and JKR elastic modulus (bottom) in PeakForce QNM mode. Images of flat spin-coated H-PMHS films (thickness h_0 = 0.8 µm): (A) on silicon wafer A and (B) on silicone Med-4750 sheet B. Profile section analysis according to the black line shown in height images. Elastic modulus E_{mean}: mean values of image.

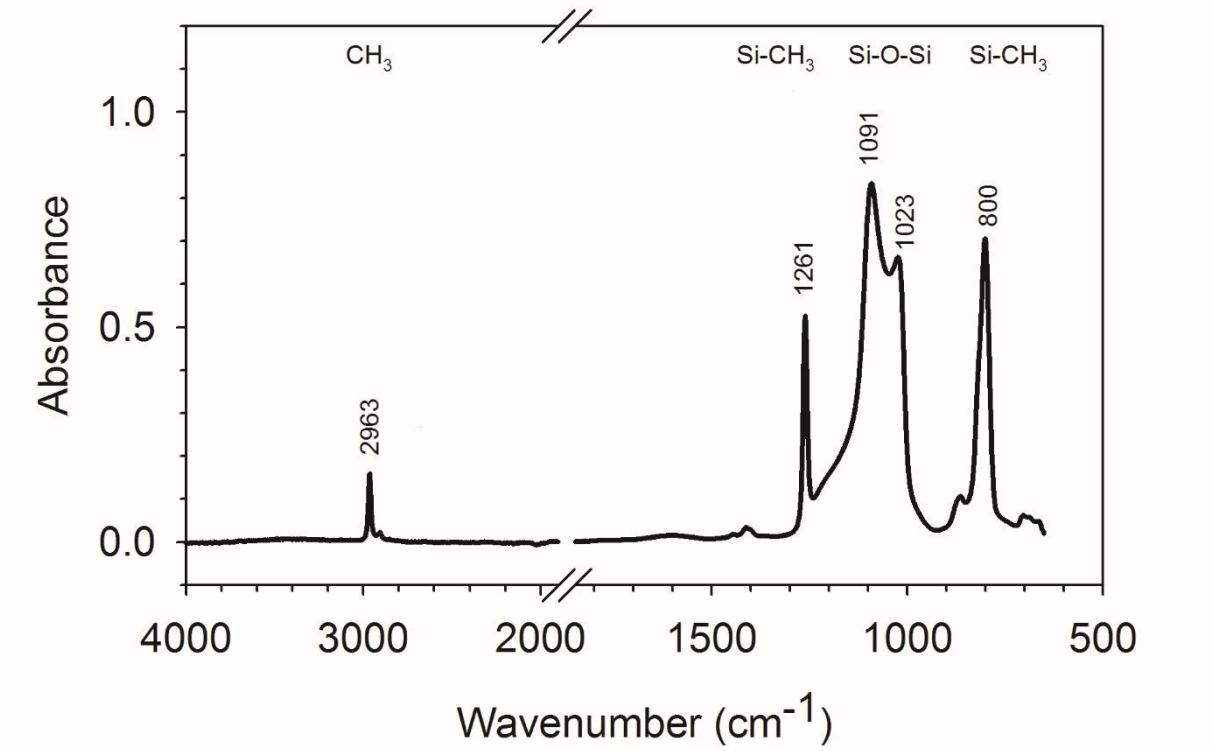

Figure S3. ATR-FTIR spectrum of the silicone elastomer Med-4750 (bare sheet) (B) and typical vibration or bending bands (cm^{-1}) assigned (upside) to poly(dimethylsiloxane) PDMS structure $[SiO(CH_3)_2]_p$. The refractive index (*n*) of PDMS of 1.4 was taken[S3] as input for the ATR correction.

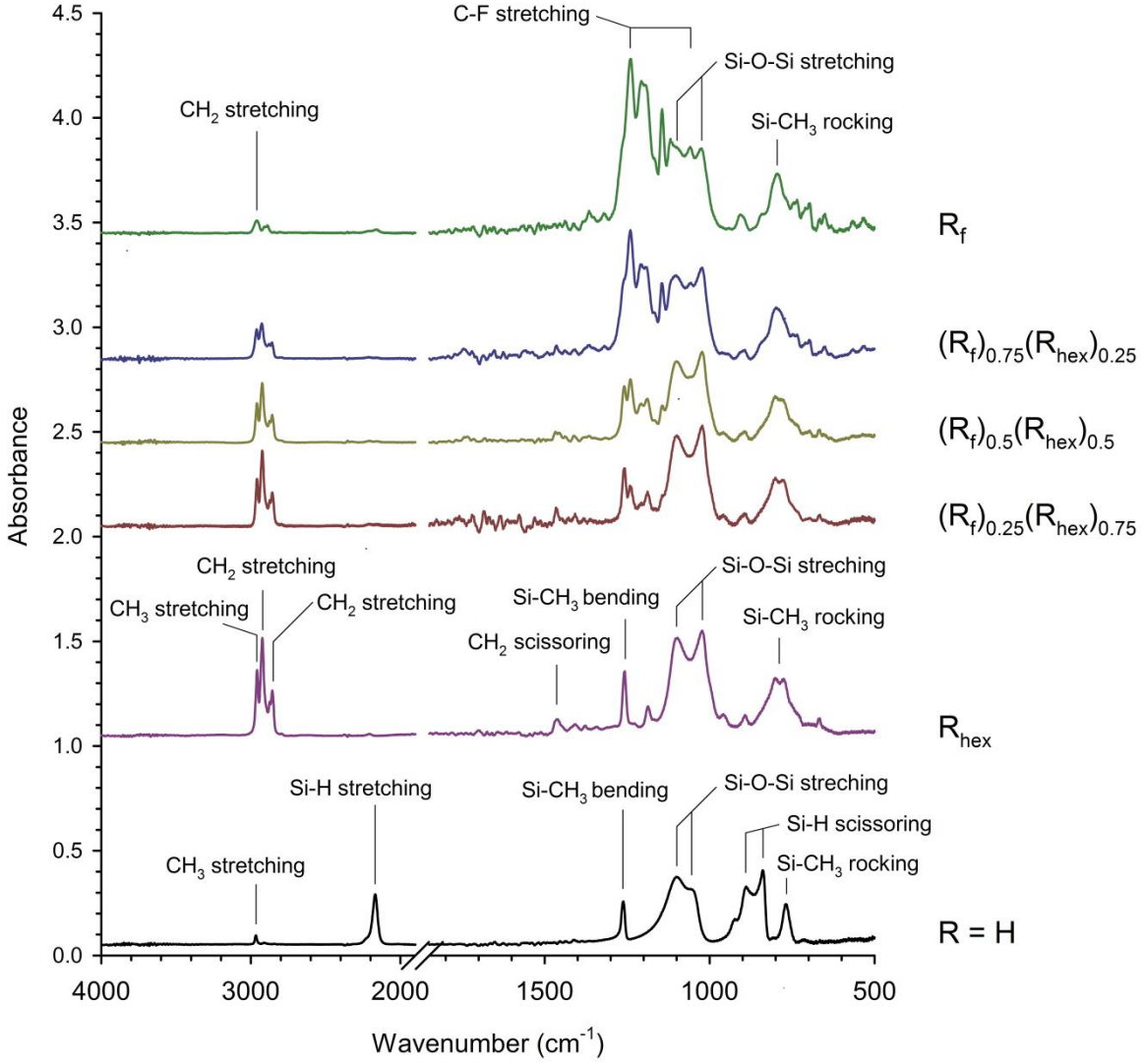

Figure S4. Transmission FTIR spectra of the evolution of R-PMHS thin films on Si wafer (A) before (R = H) and after hydrosilylation grafting $(R_f)_x(R_{hex})_{1-x}$-PMHS *versus* the molar ratio (x) = $[R_f]_0/([R_f]_0+[R_{hex}]_0)$ of alkene mixtures in the range 0 to 1 with R_f = $CF_3(CF_2)_5(CH_2)_3$- and R_{hex} = $CH_3(CH_2)_5$-. Solvents of reaction: acetonitrile, R_{hex} and R_f, and cyclohexane, $(R_f)_{0.25}(R_{hex})_{0.75}$, $(R_f)_{0.5}(R_{hex})_{0.5}$ and $(R_f)_{0.75}(R_{hex})_{0.25}$.

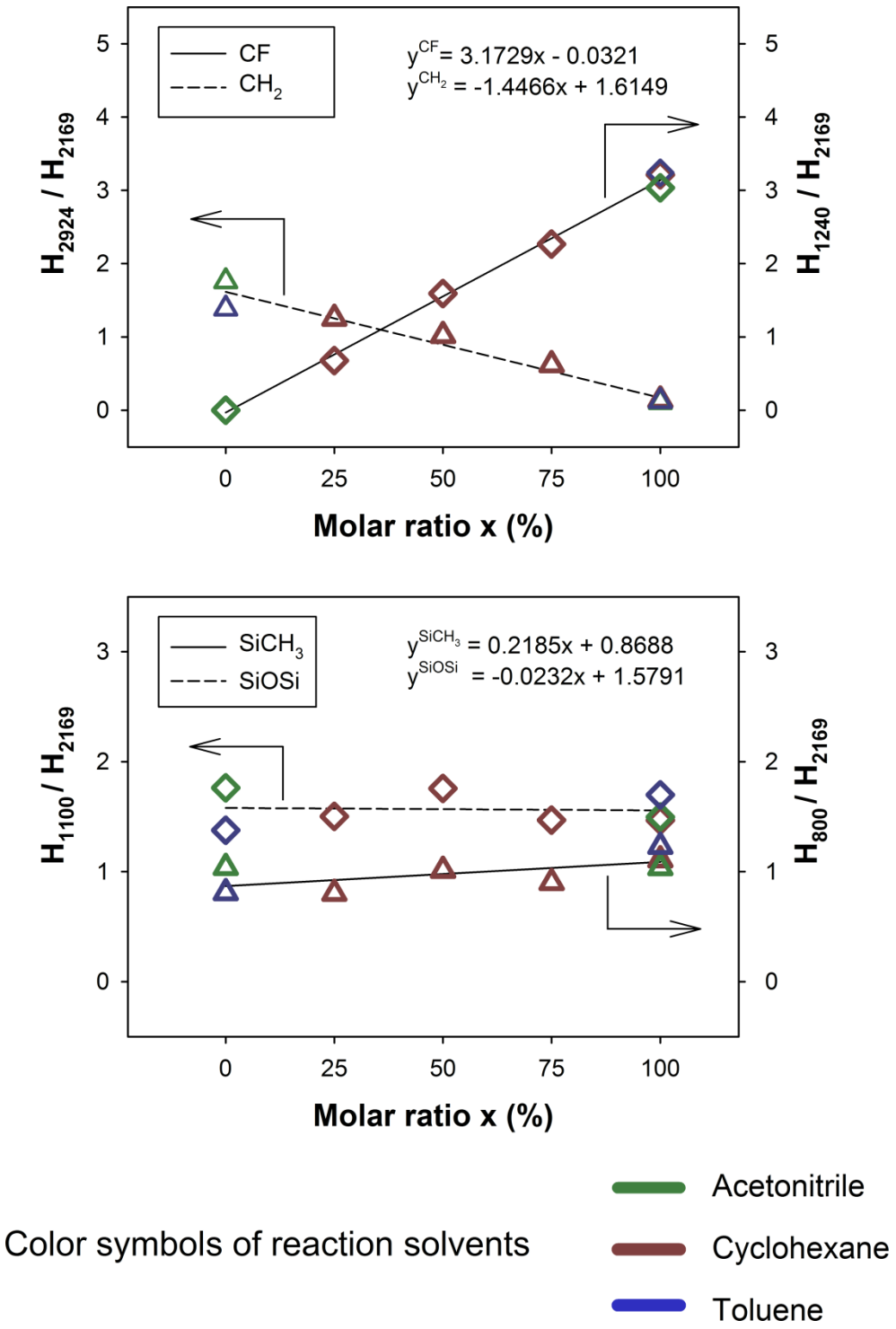

Figure S5. Calibration curves of absorbance ratio (y) H_{yyy}/H_{2169} *versus* the molar ratio (x) = $[R_f]_0/([R_f]_0+[R_{hex}]_0)$ of alkene mixtures for characteristic groups from FTIR transmission on coated Si wafers (A). H_{yyy}/H_{2169} ratio represents peak height ratio y for different vibration groups (yyy in cm^{-1}) normalized to initial SiH peak height (t = 0) at 2169 cm^{-1}, in various solvents, acetonitrile (green), cyclohexane (red) and toluene (blue).

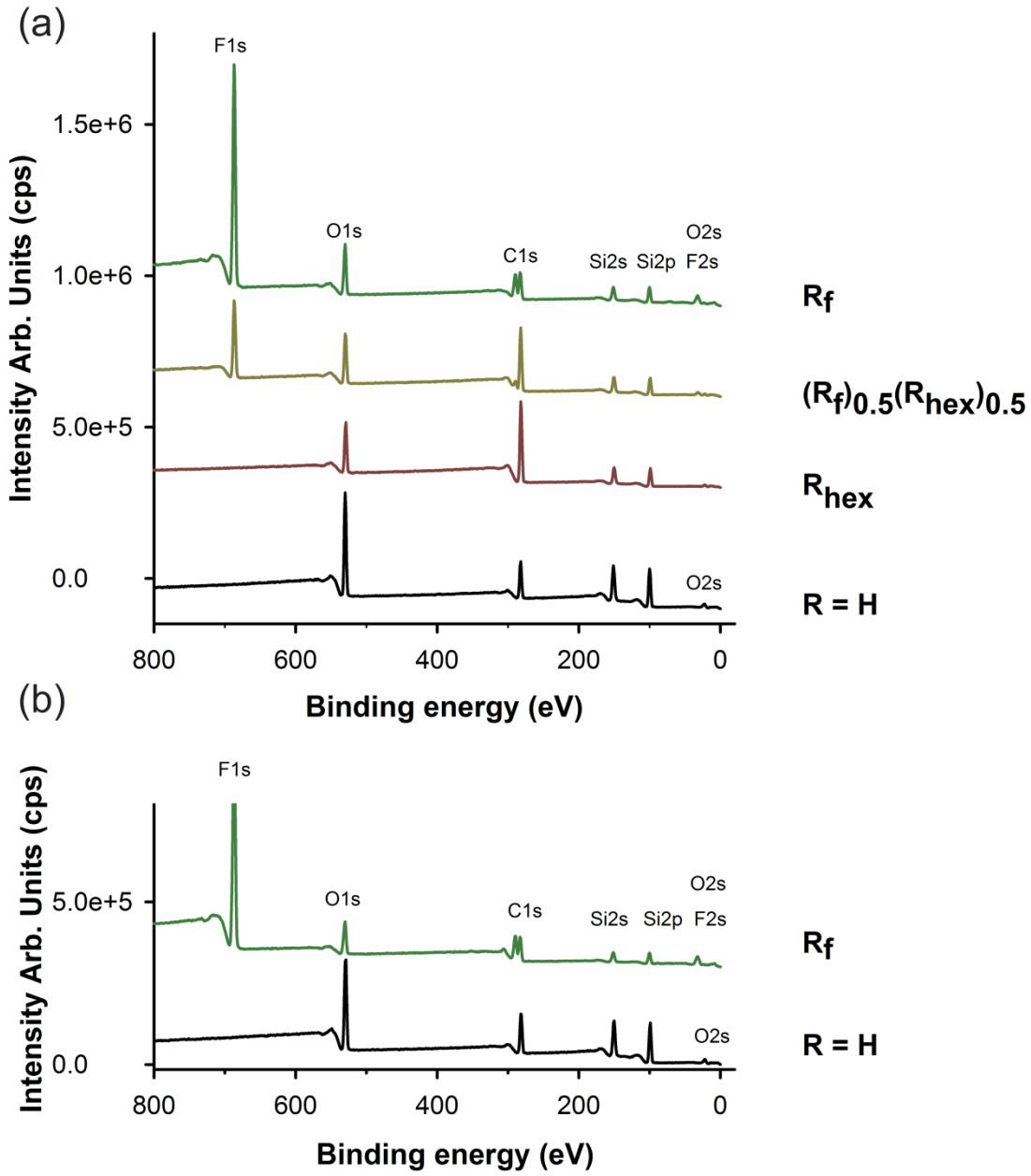

Figure S6. Typical XPS spectra of the surfaces of pristine H-PMHS thin films R = H (thickness h_0 = 0.8 µm), (a) on Si wafers A and (b) on silicone sheets B, and corresponding functionalized R-PMHS thin films: (a) R_{hex}-PMHS, R_f-PMHS and mixture $(R_f)_{0.5}(R_{hex})_{0.5}$-PMHS; (b) R_f-PMHS. Solvents of reaction: acetonitrile (x = 0, 1) and cyclohexane (x = 0.50). The corresponding surface elemental compositions (Si, C, O, F) are summarized in Table S3. The corresponding high resolution C1s and Si2p XPS spectra of (a) for R = H, R_{hex} and R_f on substrate A are given in Figure S7.

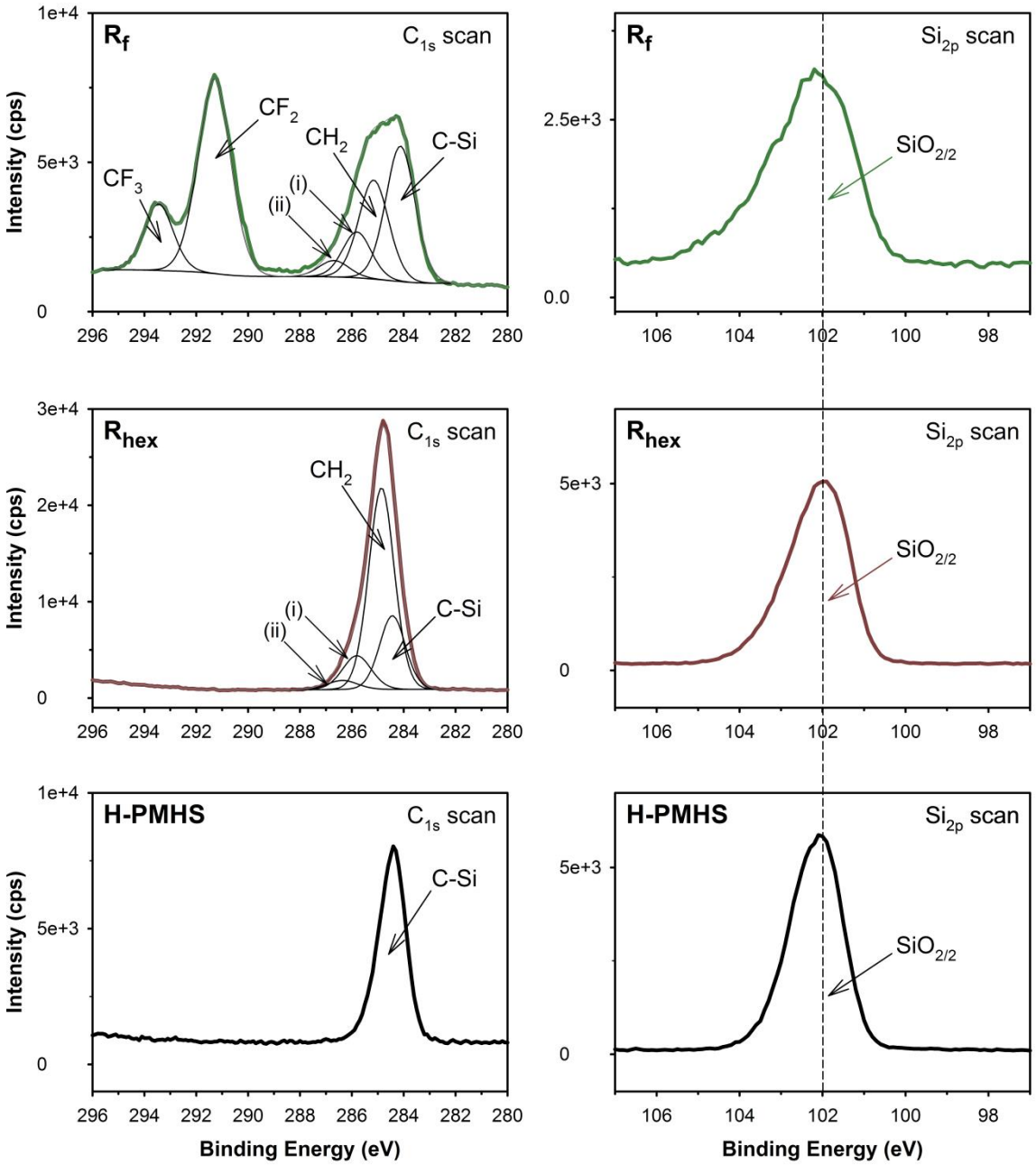

Figure S7. High resolution C1s and Si2p XPS spectra and curves fit (solid line) attributed to various chemical components for thin films H-PMHS (thickness h_0 = 0.8 µm), R_f-PMHS and R_{hex}-PMHS prepared on silicon wafers (A). Minor components (i) and (ii) attributed to C-C-O and C-O, respectively.

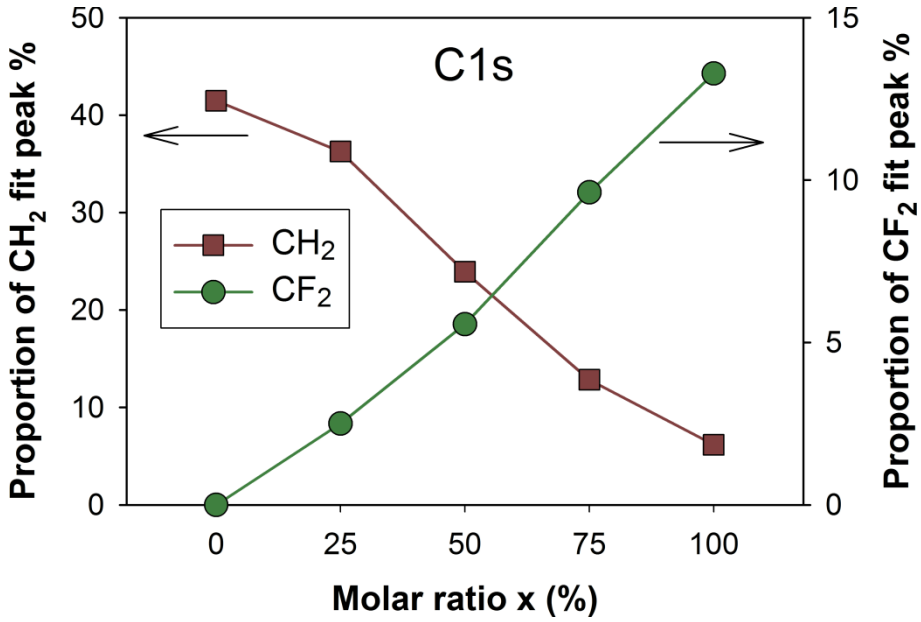

Figure S8. Evolution of $\underline{C}H_2$ and $\underline{C}F_2$ fit peaks of high-resolution C1s XPS spectra in atomic percent *versus* the molar ratio (x) = $[R_f]_0/([R_f]_0+[R_{hex}]_0)$ of alkene mixtures for the functionalized R-PMHS thin films on silicon wafer A. The proportions CH_2% and CF_2% are obtained by curve fitting of C1s spectra of various mixtures (x) in the range between 0 and 1 by increment of 0.25. Two examples of C1s deconvolution and curve fitting are supplied in Figure S7 for films R_{hex}-PMHS and R_f-PMHS.

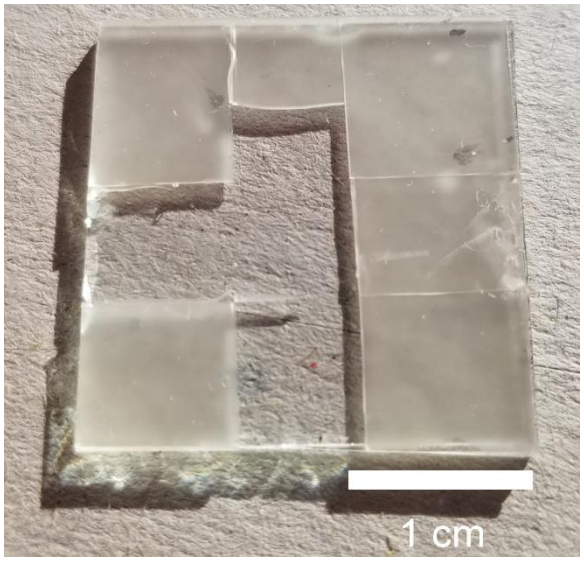

Figure S9. Picture of opaque surface R_f-PMHS of roughness 0.35 µm determined by PF-QNM height image (Figure 4B). Some parts of the silicone film (transparent region) were cut and film was removed from the glass side. Sample prepared in two steps (Figures 1-2): (*i*) spin-coating of H-PMHS (thickness h_0 = 0.8 µm) on silicon Med-4750 sheet (B) supported on glass slide and (*ii*) reaction of H-PMHS film by hydrosilylation of fluorinated olefin $CF_3(CF_2)_5CH_2$-CH=CH_2 (**2**) at 65 °C (Solvent acetonitrile, Karstedt catalyst, time: 30 min).

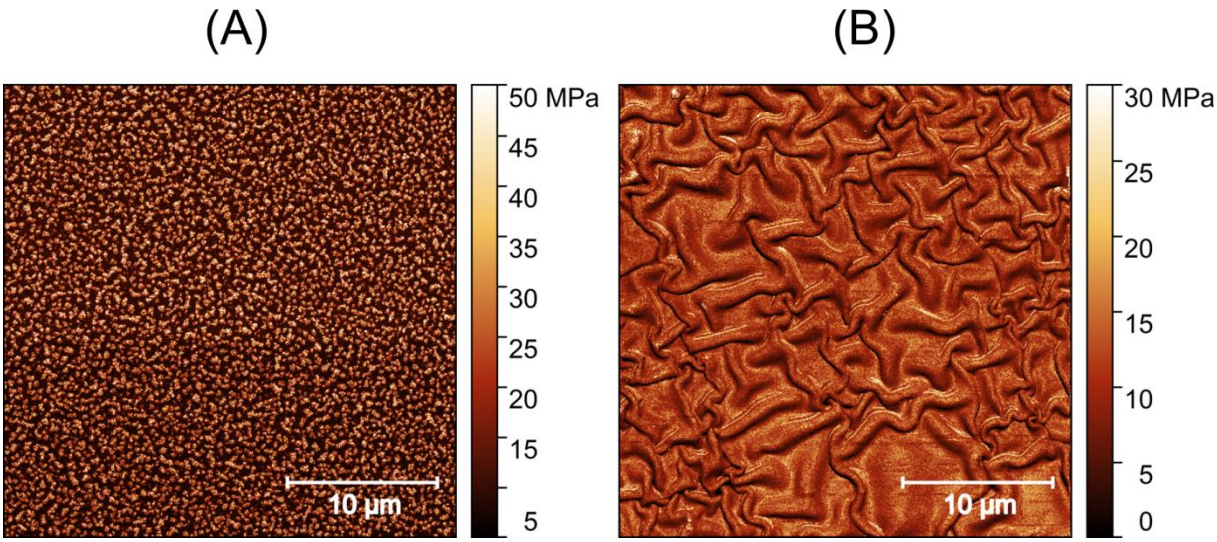

Figure S10. Representative maps of JKR elastic modulus of 30 × 30 μm^2 region in PeakForce QNM mode of corresponding height images in Figure 4 generated by swelling and hydrosilylation of 1*H*, 1*H*, 2*H*, 3*H*, 3*H*-tridecafluorononon-1-ene (**2**) with H-PMHS polymer (thickness h_0 = 0.8 μm). (A) Dotlike pattern of wavelength λ = 0.4–0.7 μm on rigid Si wafer substrate A. (B) Wrinkled pattern of λ = 4–7 μm on soft elastomeric substrate B.

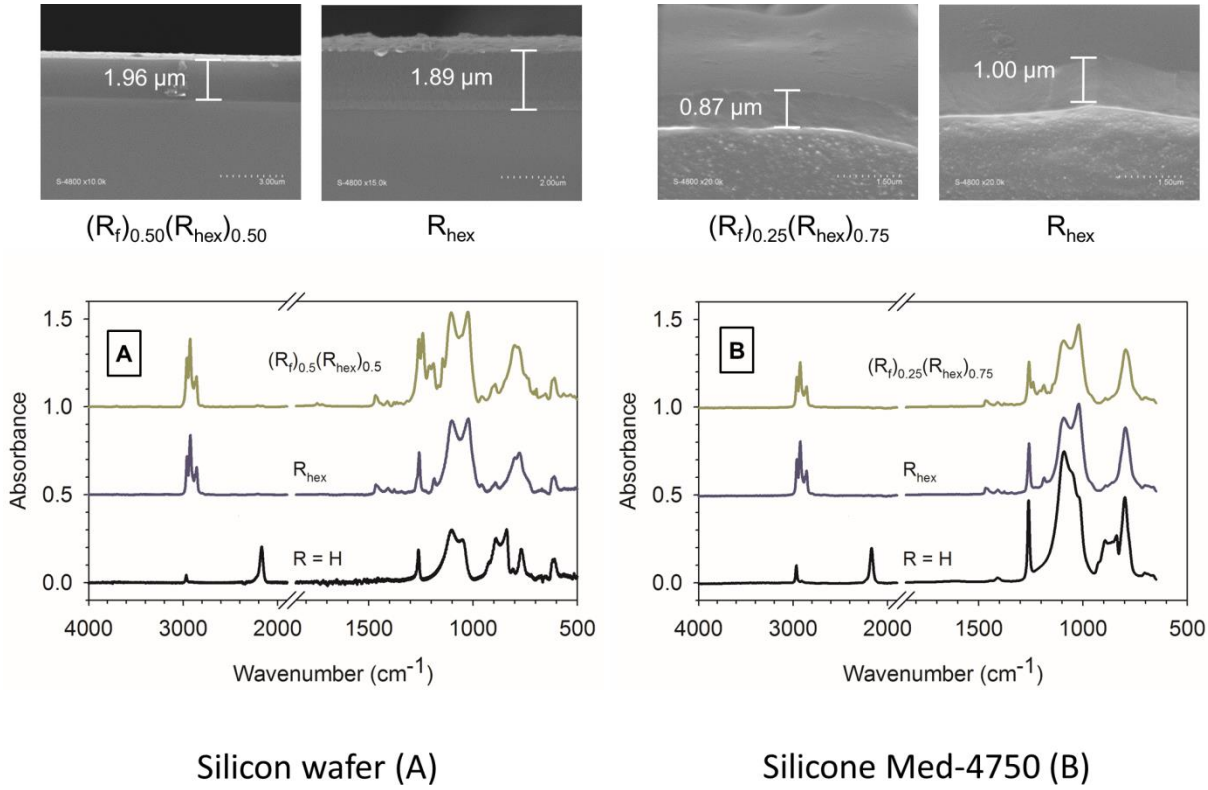

Figure S11. (Top) SEM cross-sectional view images and thickness measurement of swollen R-PMHS films after reaction with olefin mixtures of 1-hexene (**1**) and 1*H*, 1*H*, 2*H*, 3*H*, 3*H*-tridecafluorononon-1-ene (**2**) onto distinct substrates A (silicon wafer) and B (silicone Med-4750). Linear swelling ratio (α_f) from eq. 1 in main manuscript: R = $(R_f)_{0.50}(R_{hex})_{0.50}$ (2.45) and R_{hex} (2.36) on A; $(R_f)_{0.25}(R_{hex})_{0.75}$ (1.09) and R_{hex} (1.25) on B. (Bottom) Infrared spectra of pristine spin-coated H-PMHS thin film of same thickness (h_0 = 0.8 µm) and R-PMHS after functionalization *via* catalytic hydrosilylation (same sample) for sample films anchored on distinct (A) and (B) substrates, in transmission mode and ATR mode, respectively.

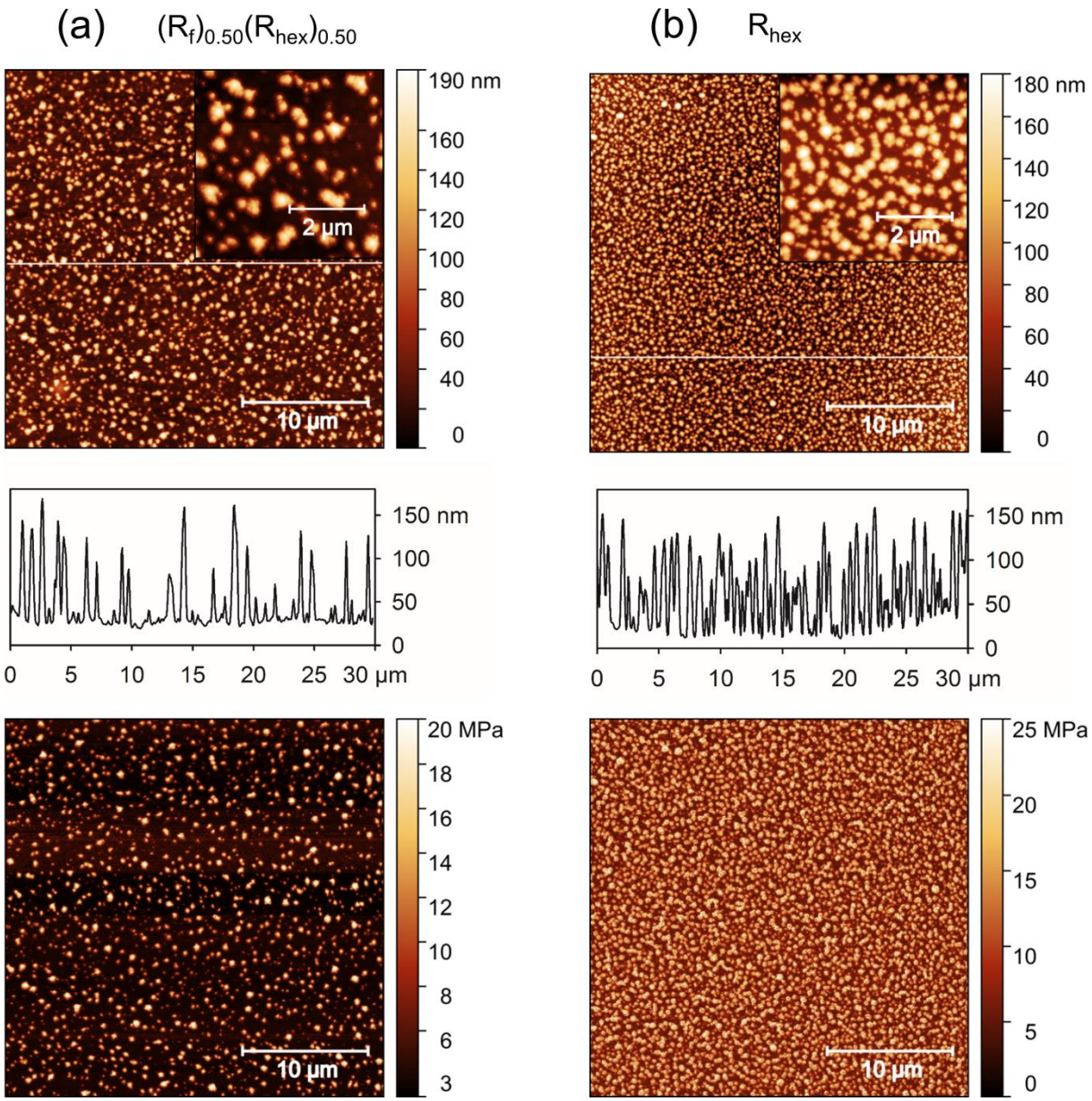
(a)
$(R_f)_{0.50}(R_{hex})_{0.50}$
(b)
R_{hex}
2 μm
10 μm
190 nm
160
140
120
100
80
60
40
0
180 nm
150 nm
50
0 5 10 15 20 25 30 μm
20 MPa
18
16
14
12
10
8
6
3
25 MPa
20
15
5

Figure S12

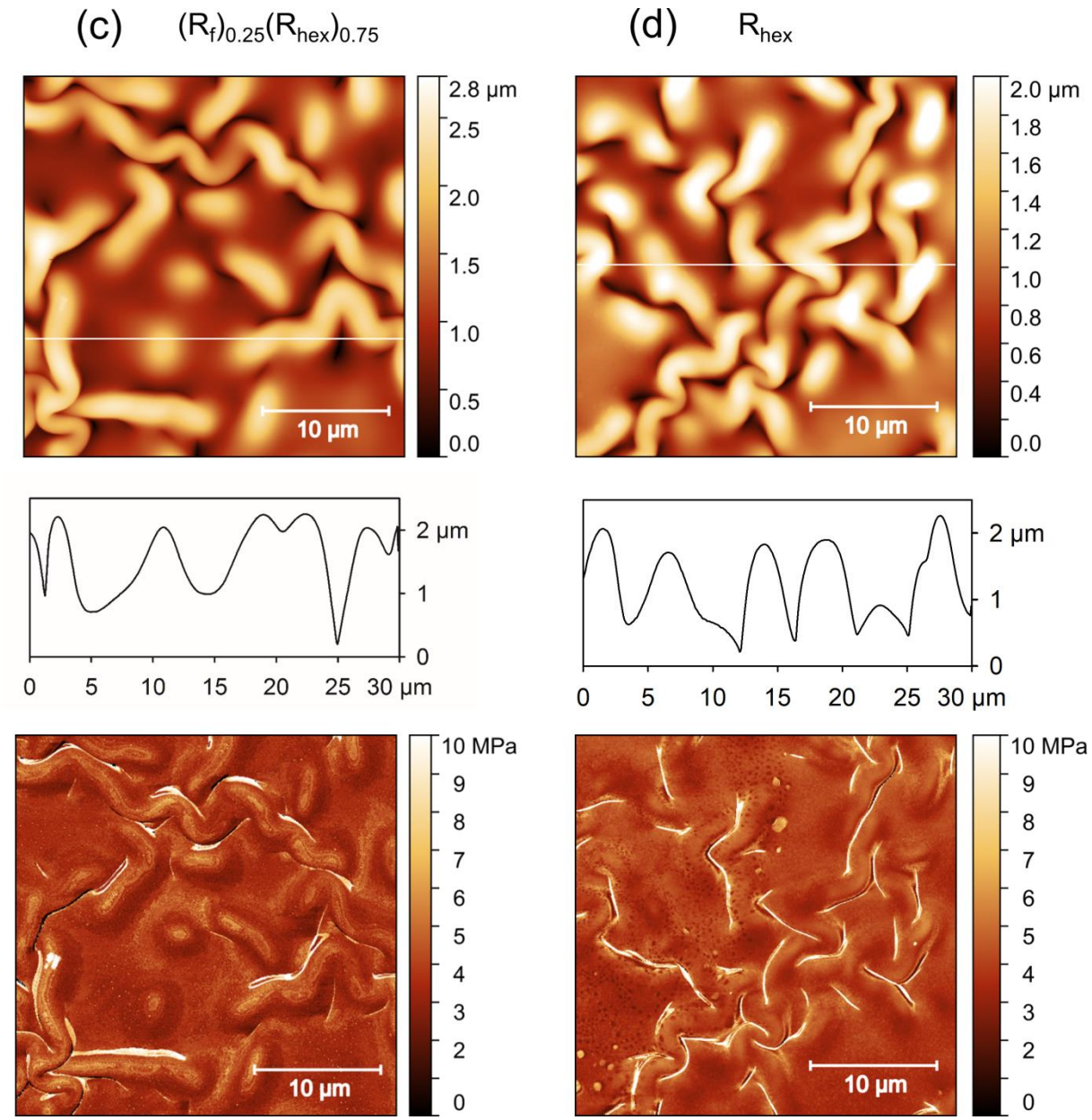

Figure S12. Representative maps of topography (Top) and JKR elastic modulus (Bottom) of 30 × 30 µm^2 region in PeakForce QNM mode of random and inhomogeneous micro patterns generated by swelling and hydrosilylation of olefin mixtures of 1-hexene (**1**) and *1H, 1H, 2H, 3H, 3H*-tridecafluorononon-1-ene (**2**) with H-PMHS polymer (thickness h_0 = 0.8 µm). Swollen R-PMHS films after hydrosilylation of olefin mixtures: (a) $(R_f)_{0.50}(R_{hex})_{0.50}$-PMHS and (b) R_{hex}-PMHS on Si wafer (A) with map insets of 5 × 5 µm^2 region; (c) $(R_f)_{0.25}(R_{hex})_{0.75}$-PMHS and (d) R_{hex}-PMHS on silicone Med-4750 (B). Profile section analysis according to the white line shown in height images.

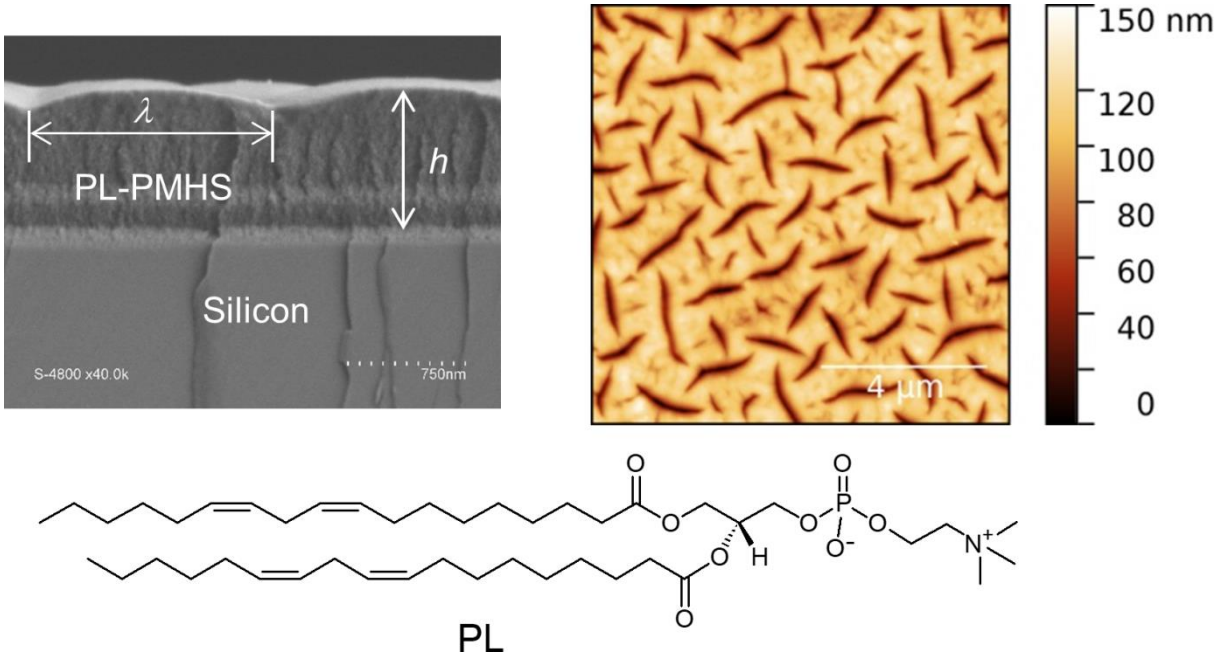

Figure S13. Surface creasing of swollen PL-PMHS film prepared by hydrosilylation of an unsaturated phospholipid molecule 1,2-dilinoleoyl-*sn*-glycero-3-phosphocholine (18:2 Cis) (PL) with spin-coated pristine H-PMHS (thickness h_0 = 0.5 µm) anchored onto (100) silicon wafer.[S4,S5] PL-PMHS fold pattern (λ ≈ 1.5 µm, h = 0.9 µm; linear swelling ratio α_f = 1.8) generated from the swelling by solvent casting in toluene and reaction of the PL precursor: (Left) SEM cross-sectional view image and (Right) atomic force microscopy top view image.

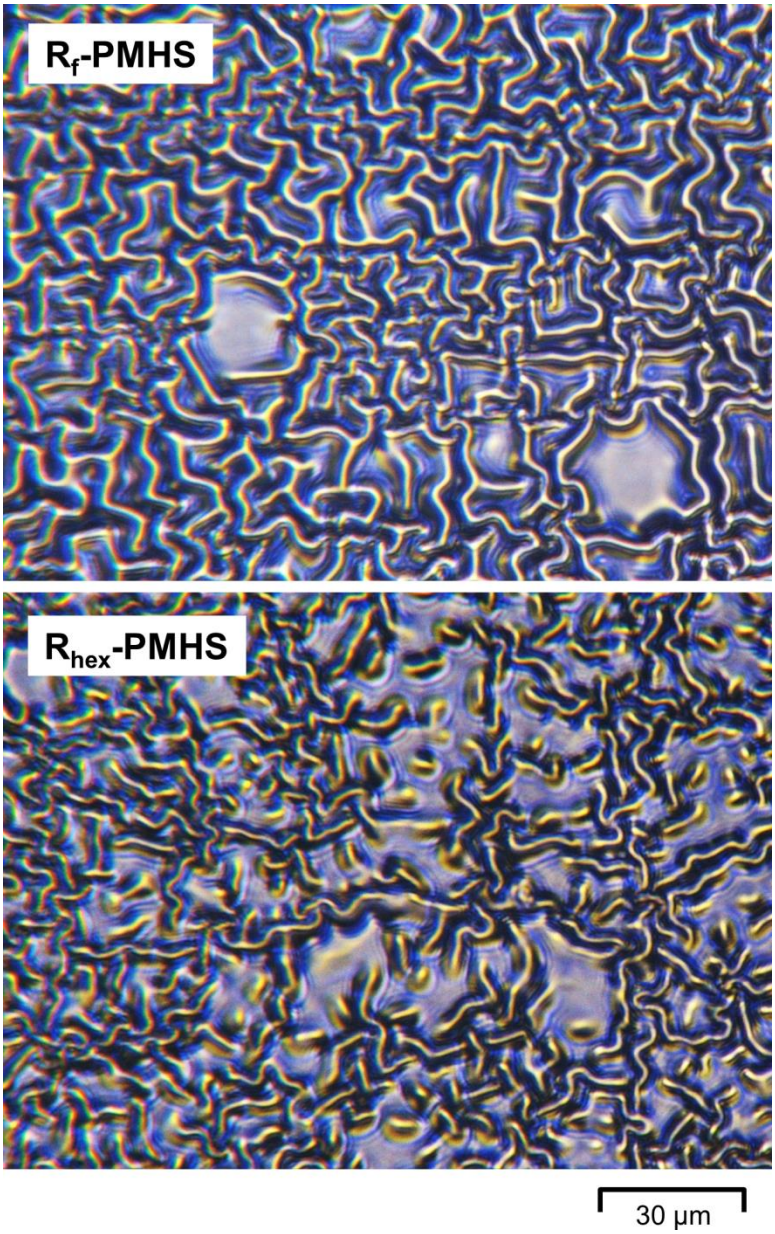

Figure S14. Surface wrinkling of swollen R-PMHS films (R = R_f or R_{hex}) after reaction at 65 °C with 1*H*, 1*H*, 2*H*, 3*H*, 3*H*-tridecafluorononon-1-ene (**2**) or 1-hexene (**1**) on silicone Med-4750 sheet (B) supported to a microscope glass slide, from optical microscopy images taken in transmission mode. Wrinkling wavelengths are λ = 4–7 µm for R_f-PMHS (Top) and λ = 4–5 µm for R_{hex}-PMHS (Bottom) patterns. The grafting alkyl chains have the molecular formulae R_f = $CF_3(CF_2)_5(CH_2)_3$- and R_{hex} = $CH_3(CH_2)_5$-.

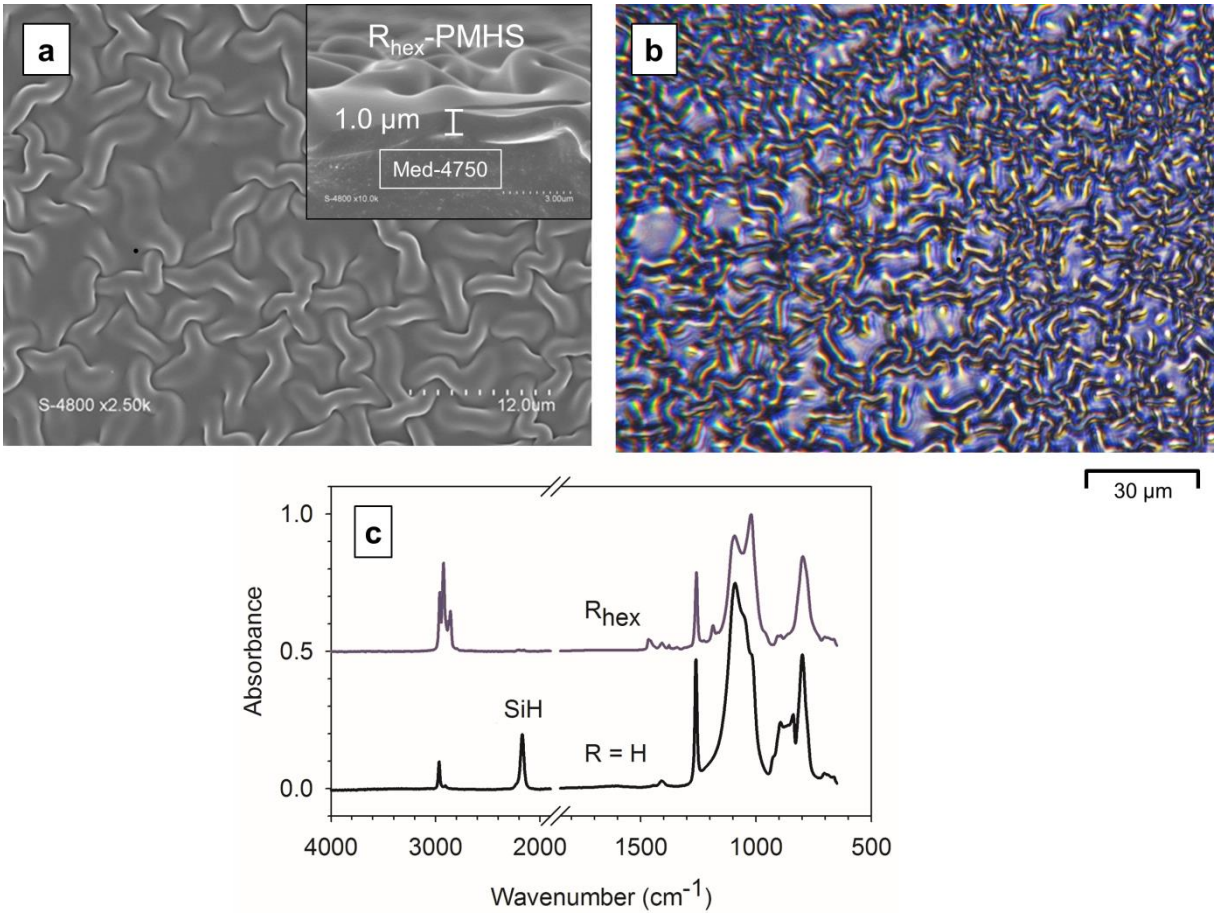

Figure S15. Surface wrinkling of swollen R_{hex}-PMHS film (thickness h = 1.0 µm) resulting from hydrosilylation of 1-hexene at room temperature in acetonitrile for 30 min onto silicone Med-4750 substrate (B). Linear swelling ratio α_f = 1.25; thickness of pristine H-PMHS thin film h_0 = 0.8 µm. (a) SEM top view and cross-sectional view images (Inset: 4× magnification image). (b) Optical microscopy image taken in transmission mode. (c) FTIR-IR spectra in ATR mode of PMHS films, before (Bottom, R = H) and after reaction (Top, R = R_{hex}).

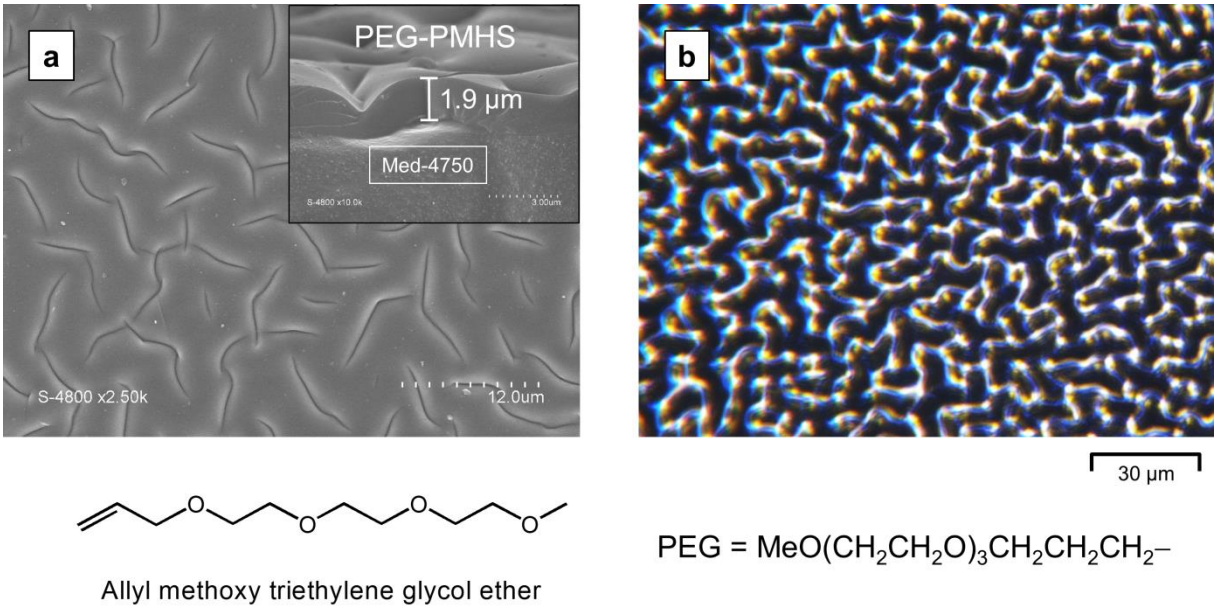

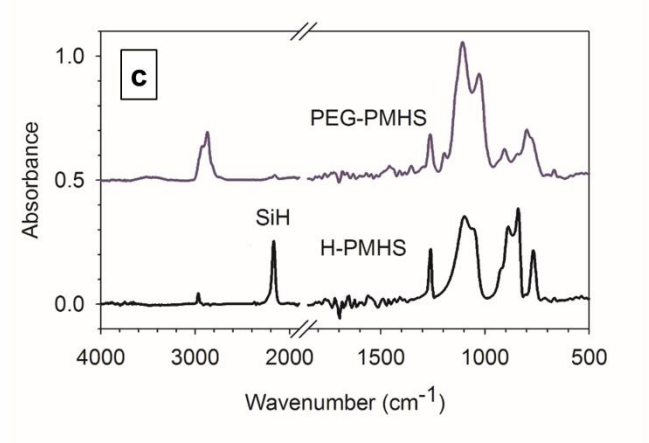

Figure S16. Surface creasing of swollen PEG-PMHS film film (thickness h = 1.9 μm) resulting by hydrosilylation of allyl methoxy triethylene glycol ether at 40 °C in acetonitrile for 30 min onto silicone Med-4750 substrate (B). Linear swelling ratio α_f = 2.4; thickness of pristine H-PMHS thin film h_0 = 0.8 μm. (a) SEM top view and cross-sectional view images (Inset: 4× magnification image). (b) Optical microscopy image taken in transmission mode. (c) FTIR spectra in transmission mode of PMHS films, before (Bottom H-PMHS) and after reaction (Top PEG-PMHS) prepared in similar conditions on Si wafer (A).

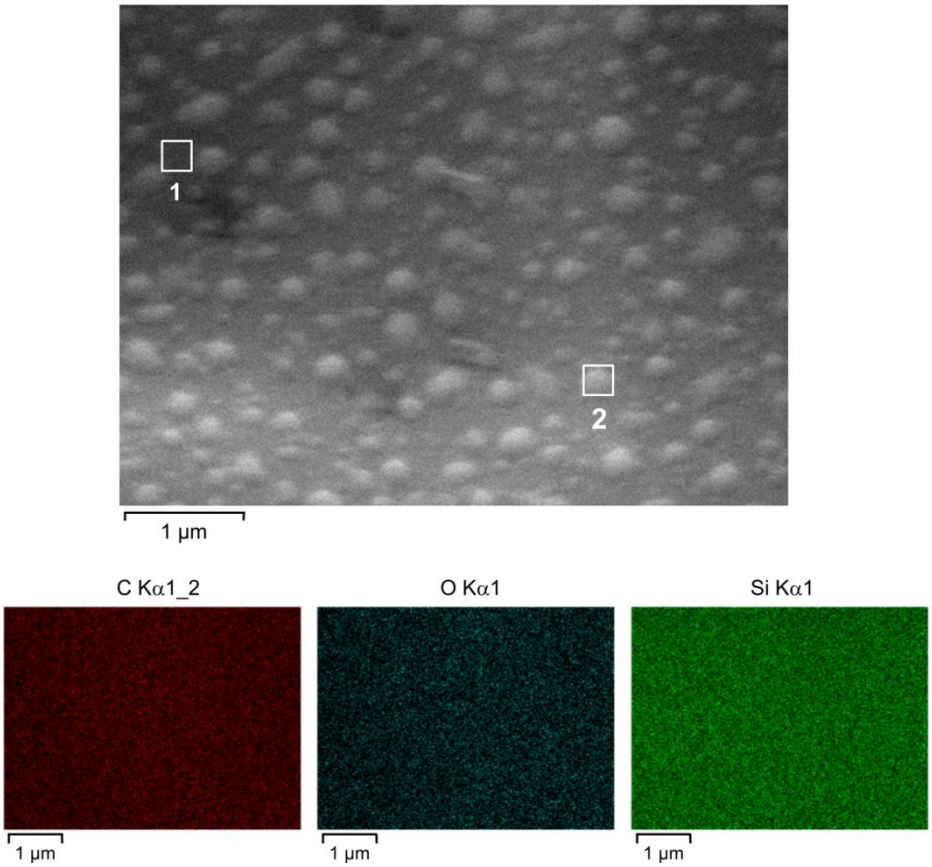

Figure S17. Energy Dispersive X-ray spectroscopy (EDX) of the functionalized polymer R_{hex}-PMHS film (h = 1.9 µm) on Si wafers (A). (Top) Electronic image of the dotlike pattern generated on R_{hex}-PMHS top film. The white squares are typical scanned regions of surface areas 0.25 µm × 0.25 µm analyzed by EDX corresponding to flat (1) or rough (2) zones, with and without peak zone, as summarized in Table S6. (Bottom) Typical maps of the corresponding EDX scanned surface for carbon, oxygen and silicon elements.

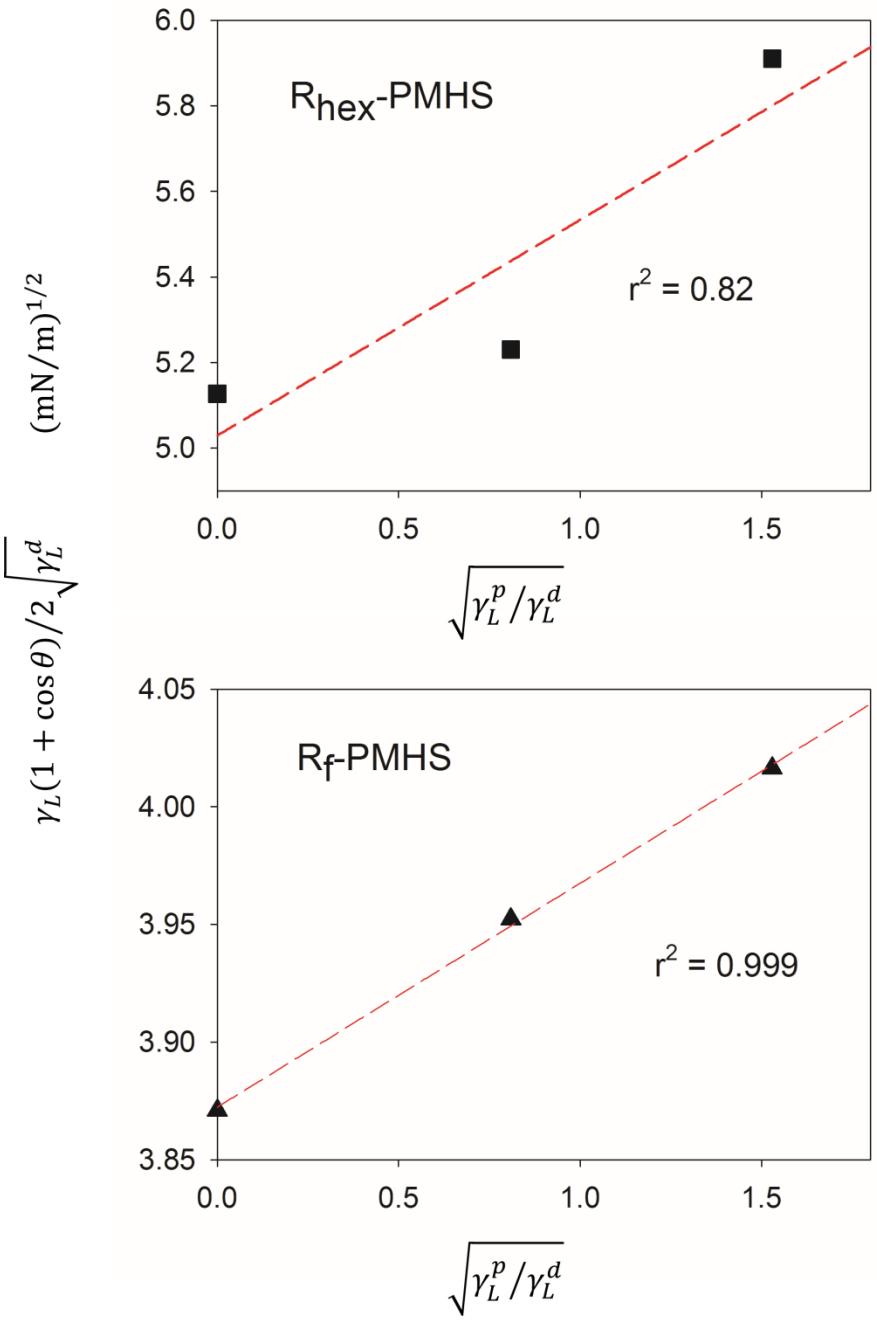

Figure S18. Plot of $\gamma_L(1+\cos\theta)/2\sqrt{\gamma_L^d}$ *versus* $\sqrt{\gamma_L^p/\gamma_L^d}$ by measuring the contact angle θ of different liquids (water, ethylene glycol and *n*-hexadecane) against R-PMHS solid, derived using the values of dispersive γ_L^d and polar γ_L^p components of the surface energy of the liquids listed in Table S7, according to the Owens and Wendt's method.[S1] The data were fitted to the dotted red line. The dispersive γ_S^d and polar γ_S^p components of the surface energy of the

solid can be calculated from the slope and intercept of the regression line using equation S14 (Section 6): The square of the intercept in the Y-axis yields the value of γ_S^d as 25.3 mN/m (R_{hex}-PMHS) and 15.0 mN/m (R_f-PMHS), and the square of the slope yields the value of γ_S^p as 0.3 mN/m (R_{hex}-PMHS) and 0.01 mN/m (R_f-PMHS). The R-function has the molecular formulae: R_{hex} = $CH_3(CH_2)_5$- and R_f = $CF_3(CF_2)_5(CH_2)_3$-. The detailed results of calculation are summarized in Table S8.

Discussion

1. **Thin Films Preparation and Chemical Modification**

The nomenclature of the films prepared on two distinct substrates silicon wafer (A) and flat silicone elastomer Med-4750 sheet (B) is summarized in Table S1.

1.1. Cleaning of Substrates

1.1.1. Silicon Wafer

Prior to thin film deposition, the native oxide silica (thickness ≈ 2 nm) of silicon wafer (A) was activated by UV/Ozone oxidation process (UVO) in order to increase the density of surface hydroxyl groups of silica. Thus, pre-cleaned wafer samples were placed under a photosensitized lamp (Hg vapor) for 15 min within 5 mm of the radiation source (UVO-Cleaner with an ozone killer system, Jelight 42, USA).

1.1.2. Silicone Elastomer Med-4750

The topography and nanomechanical properties of the Med-4750 sheet (B) were determined as received by PF-QNM microscopy (Figure S1). Before depositing the H-PMHS layer, the silicone elastomer Med-4750 was first washed thoroughly with isopropanol, then dried under a stream of nitrogen and finally at 70 °C for 10 min. Prior to thin film deposition, the silicone

pieces were hold on UVO cleaned microscope slides by just placed on them with gentle pressure.

1.2. Synthesis of Crosslinked H-PMHS Films

1.2.1. Silicon Wafer

The protocol for the synthesis of 5% crosslinked pristine H-PMHS thin films by spin-coating sol-gel solution on silicon wafer (100) substrates is described elsewhere.[S4-S7] Briefly, methyldiethoxysilane/triethoxysilane 95/5 (mol %) mixture of silane monomers (silane concentration [Si] = 4.0 M) in EtOH (molar ratio [EtOH]/[Si] = 1) with triflic acid ($[CF_3SO_3H]/[Si]$ = 0.05%) was polymerized by addition of water with hydrolysis ratio $[H_2O]/[SiOEt]$ = 0.5. The freshly activated substrate was purged in the spin-coater (Spin150, SPS Europe) for 2 min under a stream of argon (2 L/min) to avoid ambient air moisture. The resulting clear sol was allowed to age at room temperature for about 30 minutes, then filtered and deposited to totally cover the main face of the piece before starting rotation after 10 s. The spin coating was performed with rotational speed of 4000 rpm (spin acceleration of 2000 rpm/s) and rotation time was fixed at 30 s. The coated samples were allowed to cure at room temperature (22 °C) for 1 hour and finally at 110 °C for 10 minutes giving very smooth H-PMHS films of roughness R_q = 2.5 nm (Figure S2) and of thickness $h_0 \approx$ 0.8 µm as measured by transmission IR spectroscopy (Section 1.2.3).

1.2.2. Silicone Elastomers Med-4750

The sol-gel liquid precursor as described for wafer may also be used for spin-coating to prepare pristine PMHS films on smooth silicone Med-4750 pieces (IR spectra in Figure S3) of roughness R_q = 40 nm (Figure S1). The spin-coating process was carried out under the same conditions as those used for the wafer (4000 rpm, time: 30 s) giving also very smooth film of similar thicknesses h_0 = 0.8 µm (Section 1.2.3) and of roughness R_q = 2.9 nm (Figure S2). The

H-PMHS polymer was allowed to cure at 22 °C for *ca.* 1 hour and finally at 110 °C for 10 minutes.

1.2.3. Assessment of H-PMHS Film Thickness from IR Spectra

The SiH peak was used to determine the thickness of the pristine H-PMHS films (h_0) (5% crosslinked) in IR transmission mode on silicon wafer (A) by using the absorbance peak A_{2169} at 2169 cm^{-1} for the characteristic Si–H stretching vibration:

$$A_{2169} = \alpha h_0 \qquad \text{(S1)}$$

where the calibrated value of the absorption coefficient (α) was 0.27 μm^{-1}. Equation S1 is similar to that of Beer–Lambert law in the thin films approximation.[S8] Such a calibration coefficient α was determined from the peak absorbance at 2169 cm^{-1} of a 200-nm thick sample carefully prepared onto silicon wafer by spin-coating for which independent thickness could accurately be measured using ellipsometry (Estimated accuracy of ± 5%). The thickness of starting spin-coated PMHS films on substrate (A) of 0.8 µm was then determined (Mean value of at least 5 spin-coated samples; SD ± 3%). To confirm the calibration in the micrometer range, the thickness was measured from the cross section using scanning electron microscopy (Hitachi S-4800).

On the other hand, the SiH peak height at 2169 cm^{-1} was used to control the amount of H-PMHS polymer spin-coated on flexible silicone Med-4750 substrate (B) by ATR technique. The thickness calculation, after ATR correction, gave fairly good results in agreement with MEB thickness measurements (Figure 3). This approach enables fast and simple evaluation of film thickness of H-PMHS (h_0) on substrate B because its value was below the probed depth of ATR technique (see below eq. S2). The thickness accuracy was estimated to be ± 20% including an error due to the variations of clamping force (pressure) to ensure the contact

between sample and crystal. Moreover, the silicone substrate (B), $[SiO(CH_3)_2]_p$, is transparent to IR-light in the SiH region, as evidenced by corrected ATR spectrum (Figure S3). Substrate B has also strong typical bands overlapping with those of H-PMHS (Table S2) such as CH_3 at 2963 cm^{-1}, SiOSi stretching at 1091 and 1023 cm^{-1}, $SiCH_3$ bending at 1261 cm^{-1} and $SiCH_3$ rocking bands at 800 cm^{-1} (See Figure S3). Therefore, these bands strongly increased in corrected ATR spectrum of H-PMHS on substrate (B) (Figures 3, S11 and S15). This is due to the probed depth of the evanescent wave of the order of a few microns, *e. g.* d_p = 1.5 µm at 1100 cm^{-1} (n_1 = 2.40, n_2 = 1.40 and θ = 45°), according to the ATR correction which allows compensating the higher penetration depth, d_p, of the evanescent wave of longer wavelength from Eq. (S2):

$$d_p = \frac{\lambda^{IR}}{2\pi\left(n_1^2(\sin\theta_i)^2 - n_2^2\right)^{\frac{1}{2}}} \quad \text{(S2)}$$

where λ^{IR}, θ_i, n_1 and n_2 represent the light wavelength, the angle of incidence (45°) of the IR beam relative to the perpendicular of the crystal surface, the refractive indices of the diamond (n_1 = 2.4) and of the analyzed sample (n_2 = 1.40), respectively.

1.3. Alkylation of H-PMHS Films

Alkylated R-PMHS films were prepared by hydrosilylation of different amounts of 1-hexene (**1**) and *1H, 1H, 2H, 3H, 3H*-tridecafluorononon-1-ene (allyl-C_6F_{13}) (**2**) of densities 0.678 and 1.86, respectively (Table S1), with SiH groups on silicon wafer (A) or silicone Med-4750 (B) substrates (Figure 1). The alkenes were mixed in 7.5 mL of dry solvent (CH_3CN, toluene or cyclohexane for substrate A; CH_3CN or cyclohexane for substrate B) with a droplet of Karstedt catalyst in xylene solution (5 µL) containing only as little as 5×10^{-7} mol of Pt. The Pt-catalyst concentration in these solvents was 6.45 10^{-5} M. The mixture was heated at 65 °C. To this, the pristine H-PMHS-coated sample (0.8 µm thick; 5.4 µmol SiH assuming density of

H-PMHS layer of 1) was added at 65 °C for 30 min. Different solvents were tested: toluene, cyclohexane or acetonitrile (Table S1). Samples were then washed thrice for 5 min each time with the same solvent to remove unreacted alkenes and then dried under a nitrogen stream. The same condition was used for reaction at 22 °C for R = R_{hex} on substrate B.

2. **Infrared Spectroscopy**

2.1. Characterization of Crosslinked H-PMHS Films

In this study, soft elastomeric network, denoted H-PMHS, were prepared with a crosslinker ratio (1-α) of 0.95 by sol-gel process using 5% of triethoxysilane crosslinker. After reactions and drying, fully crosslinked 3D networks were formed predominantly consisting of fully condensed functional silicon $SiH(CH_3)O_{2/2}$ (D^H subunits) and $SiHO_{3/2}$ (T^H) according to ^{29}Si solid-state magic angle spinning (MAS) NMR spectra of powders.[S9] This was confirmed by XPS high-resolution Si2p spectrometry (see Section 3) and by IR spectroscopy with no SiOH and no residual SiOEt (Figure S4). The IR spectrum of H-PMHS film displays the typical SiH stretching band at 2169 cm^{-1} and bending at 839 and 890 cm^{-1} attributed to $SiH(CH_3)O_{2/2}$ (D^H) units in polysiloxane segment.[S7,S9,S10] The average mesh size of the 3D network in thin film was characterized by, *N,* the average number of monomer units in PMHS segment $[SiHCH_3O_{2/2}]_N$ between two crosslinkers (Figure 1). This reference value was calculated from eq. S3 derived from simple geometric consideration by neglecting the formation of cycle:

$$N = 2\alpha/f(1-\alpha) \qquad \text{(S3)}$$

where $f = 3$ is the functionality of the crosslinker and (1-α) the crosslinker ratio (α = 0.95, $N \approx 13$, M ≈ 780 g/mol per segment). Their spin-coated film thicknesses (h_0) need to be evaluated by SEM measurement and IR spectroscopy on both (A) and (B) substrates to allow suitable evaluation of the linear swelling ratio of the film ($\alpha_f = h/h_0$) after hydrosylilation of olefins (See details in Section 1.2.3). Their average IR thicknesses, h_0, were found *ca.* 0.8 µm

for both substrates, which were also confirmed by the SEM measurement from cross-sectional view pictures (Figure 3).

2.2. Characterization of Grafted R-PMHS Films after Hydrosilylation

2.2.1. Sample Films Prepared on Substrates (A) and (B) in Acetonitrile

Hydrosylilation of 1-hexene (**1**) or *1H, 1H, 2H, 3H, 3H*-tridecafluorononon-1-ene (**2**) (Figure 1) were performed with H-PMHS thin films by immersion in alkene solutions (3.3 % v:v) giving quantitative results using Karstedt catalyst as evidenced by the vanishing of SiH stretching band of H-PMHS at 2169 cm^{-1} (Figure 3). When the sample was immersed in solution using acetonitrile which is a poor swelling solvent for silicone, the olefins subsequently diffused into the bulk of H-PMHS layer because of their hydrophobic nature. In addition, monitoring the reaction showed that the grafting of H-PMHS was achieved in only a few dozen of minutes in air at 65 °C within the H-PMHS network of 0.8 µm thick. These conditions were adopted for all experiments using the fluorinated alkene in order to favor the reaction/diffusion. After reaction, the IR spectra of the total product mixture (Figure 3) show that the strong Si–H absorption peaks almost disappeared concomitantly to the presence of those of CH_2 groups for hexyl chains (2924 and 2857 cm^{-1}) and CF groups for fluoroakyl chains (1240, 1207, 1191 and 1144 cm^{-1}) (Table S2).

2.2.2. Sample Films and Mixtures Prepared on Substrates (A) in Various Solvents

Further investigation by varying the molar ratio (x) of R_f chain with respect to R_{hex} chain was achieved by immersing H-PMHS anchored film on Si wafer substrate (A) into alkenes mixture containing *1H, 1H, 2H, 3H, 3H*-tridecafluorononon-1-ene and 1-hexene (Table S1). The resulting $(R_f)_x(R_{hex})_{1-x}$-PMHS films were characterized by using FTIR spectroscopy in transmission mode where the alkene molar ratio (x) was in the 0 to 1 range by step of 0.25 (Figure S4). The main characteristic bands of modified H-PMHS in the 400–4000 cm^{-1} region are shown in Table S2. The grafting yield (ρ) of hydrosilylation was defined by the

conversion of characteristic SiH stretching band at 2169 cm^{-1} and was quasi-quantititative ($\rho \approx 95-100\%$) for series of experiments with alkenes mixtures *1H, 1H, 2H, 3H, 3H*-tridecafluorononon-1-ene (*x*) and 1-hexene (1–*x*), in solvents such as toluene, cyclohexane and acetonitrile (Figure S4). The reaction in the 3D network thin film is expected to produce the [$R(CH_3)SiO_{2/2}$]/"D" units and [$RSiO_{3/2}$]/"T" units in R-PMHS according to a previous study performed with 1-dodecene using solid state ^{29}Si and ^{1}H NMR techniques.[S7]

To analyze the degree of functionality after reaction *versus* the molar ratio (*x*) for the series of alkyl films R-PMHS, four relevant IR bands (*y*) were used at 2924, 1240, 1100 and 800-795 cm^{-1} (Figure S5, intensity ratios *versus x* molar ratio), attributed to CH_2, CF_2, SiOSi and $SiCH_3$ vibration groups, respectively (Table S2). This enabled to determine the H_y/H_{2169} peak intensity ratios (as height) normalized with the strong peak of SiH stretching (H_{2169}) of H-PMHS taken as an external reference.

The normalized $\varepsilon_y/\varepsilon_{2169}$ coefficients of R_{hex}- and R_f-PMHS samples deduced from the slope of these straight-lines (Figure S5) are listed in Table S2 (from a detailed calculation in section 5). The $\varepsilon_{CH2}/\varepsilon_{2169}$ coefficient of 1.61 was found for CH_2 in hexyl side chain and 0.17 for CH_2 in fluorinated side chains. In contrast, with CH_2 or CF_2 groups, both H_{SiOSi}/H_{2169} and H_{SiCH3}/H_{2169} intensities attributed to polysiloxane backbone are quasi-constant as they are not expected to change significantly with *x* value (Figure S5). These extinction coefficients were also not affected by the functionalities (R_{hex}- and R_f-) of the polymer (Table S2).

The frequency shift and shape of SiOSi doublet band patterns of series of functionalized films are similar to that of the pristine H-PMHS, as shown in Figure S4 and Table S2. The IR spectra of the films do not display any significant increase of SiOSi stretching band after reaction and no presence of broad OH band at 3500 cm^{-1}. This situation is different from that observed in previous studies, in the cases of bulkiness alkene silol precursor[S11] or hydrophilic

unsaturated phospholipid precursor,[S5] where the hydrolysis was in competition with hydrosilylation. Indeed, Pt-catalyzed dehydrocoupling side-reactions can occur between SiH/SiOH,[S12] hence leading to an increase of SiOSi band and presence of SiOH band. In that case, this would ultimately lead to new SiOSi crosslinks which should harden the polymer film. However, we cannot exclude the possibilities that some SiH groups were consumed by formation of Si-Si bonds from Si-H bonds, then leading to SiOSi by autoxidation of Si-Si, especially if the main reaction is limited by a difficult diffusion of alkene reactants in the bulk of the film. These side reactions usually release gas or bubble which have never been observed on coated thin films by hydrosylilation of alkenes.

3. **XPS Spectroscopy**

The surface chemical composition of the top layer PMHS coatings was analyzed as 1–3 µm thick films deposited on polished silicon wafer or on silicone elastomer sheet (Figure S6). The wide-scans XPS spectra confirm continuous and homogenous film coverage on both substrates. Thus, the XPS spectra reveal the characteristic signals of the elements constituting monomer moieties *i.e.* F, O, C and Si (Table S3). The spectra were calibrated using the hydrocarbon contaminant or alkane C1s peak at 284.8 eV. The C1s peak of Si–$\underline{C}H_3$ and F1s peak were found at binding energy of 284.4 eV and 689.1–688.7 eV, respectively, in agreement with standard polymers: C1s at 284.4 eV for PDMS $[Si(CH_3)_2O]_p$,[S13,S14] and F1s as expected between 690.6 eV and 688.2 eV for polytetrafluoroethylene,[S15] $(CF_2\text{-}CF_2)_p$, and poly(vinylidene fluoride),[S16] $(CH_2\text{-}CF_2)_p$, respectively. As expected, the C1s binding energies for CF_2 and CF_3 groups in fluoropolymers differ appreciably giving reliable C1s fitting results (*vide infra*, Figure S7) while the F1s binding energies in $CF_3(CF_2)_5$ chains do not differ significantly.[S17] Thus, F1s curve fitting was not achieved in this study.

The PMHS coatings prepared on Si wafers or silicone sheets have quasi-identical XPS spectra (Figures S6a and S6b) and atomic composition (Table S3), confirming the versatility of the coating process. The grafting of fluorinated alkene chain onto pristine H-PMHS top layer is clearly evidenced from XPS spectra of functionalized coatings $(R_f)_x(R_{hex})_{1-x}$-PMHS by an increase of the intensity of the characteristic signal of F1s at 689.1–688.7 eV with the molar ratio x = 0.25–1.00 (Figure 8, panel down).

To gain further insight into the structure of the polysiloxane backbone and substituents grafted on silicon atom, a more detailed evolution of Si2p and C1s high resolution spectra are evidenced in Figure S7 for three films with R = H, R_{hex} and R_f. In C1s spectrum of H-PMHS, the C–Si component can be attributed to $Si\underline{C}H_3$ carbon in the starting matrix in agreement with the value of 284.4 eV reported for bulk PDMS polymer,[S13] along with a small amount of C–C contribution at 285.2 eV assigned to organic contaminant (not shown in Figure S7 for clarity). In C1s spectrum of fluoroalkyl film R_f-PMHS, the signal can be well-fitted with three main characteristic components with binding energies given in Table S4: (*i*) The $\underline{C}F_3$ and $\underline{C}F_2$ components are typically characterized by a C1s peak ratio (as peak area) of 5 (Table S3) in good agreement with the perfluoroalkyl structure $CF_3(CF_2)_5$-.[S18] (*ii*) The C–C component is attributed to CH_2 in $CF_3(CF_2)_5$–$(CH_2)_3$–Si≡ adduct. (*iii*) The $\underline{C}$–Si component is assigned to both $Si\underline{C}H_3$ and $Si\underline{C}H_2$ groups attached to the silicone backbone. Indeed, the C1s binding energy of $\underline{C}$–Si bonds is expected to be relatively insensitive to alkyl substitution in alkyl polysiloxane.[S19] XPS spectra confirmed the good reactivity of the allyl type fluorinated olefin onto pristine H-PMHS which yields the linear fluoroalkyl adduct $CF_3(CF_2)_5$–$(CH_2)_3$–Si≡ resulting from the anti-Markonikov rule.[S20] XPS spectrum of R_{hex}-PMHS confirmes the C1s peak which can be well-fitted by two major components, $\underline{C}$–Si and CH_2 (major contribution), in agreement with the expected $CH_3(CH_2)_5$–Si≡ structure of grafted chains. The percentages of CH_2 and CF_2 components were determined from C1s curve-fitting *versus* the alkenes molar

ratio *x* (*x* = 0 to 1.00 by step of 0.25) (Figure S8). These plots confirmed the formation of grafted polysiloxane with fine-tuned functionality in agreement with IR results.

The Si2p high resolution spectra of PMHS polymers (Figure S7) display only one major component peak attributed to difunctional D^R or D^H silicone units for linear segments in networked polymers (Figure 1). The values of binding energies are comparable, 102.1, 102.0, 102.0 and 102.1 eV (± 0.2 eV), for R = H, R_{hex}, $(R_{hex})_{0.5}(R_f)_{0.5}$ and R_f, respectively, in agreement with PDMS resins:[S21] $[(CH_3)_2SiO_{2/2}]$/D units 102.0 ± 0.1 eV; $[CH_3SiO_{3/2}]$/T units 102.7 ± 0.1 eV (δ_{T-D} = 0.7 eV). Indeed, we expected the binding energy shift of D units caused by replacement of Si–H by Si–R to be small in comparison to that shift induced by oxygen between D and T units for instance (δ_{T-D} = 0.7 eV).[S14,S21] Moreover, there is no significant shift of the Si2p at higher binding energy as measured in our previous work,[S5] δ = +0.7–0.9 eV, indicating that trifunctional T-silicon units ($SiO_{3/2}$) are not created by hydrolysis in these present films. Note that the $SiO_{3/2}$ content (< 5 %) of T-crosslinker was not enough in actual spectra to give reliable results by Si2p curve-fitting. These results clearly demonstrate that the final structure of the modified polymer is similar to that of the non-modified H-PMHS backbone polymer constituted mainly by difunctional $SiO_{2/2}$ units. To conclude, the structure of the network polymers is confirmed by XPS Si2p spectra in agreement with the present FTIR study and previous ^{29}Si solid state NMR investigation of powder in the case of dodecene grafting.[S7]

The chemical composition data (Table S3) provides insight into the structure of the non-modified and modified PMHS. For pristine H-PMHS, the theoretical network composition $(SiCO_{2/2})_{0.95}(SiO_{3/2})_{0.05}$ (hydrogen excluded) summarized as $SiO_{1.025}C_{0.95}$ was in agreement with that of as prepared H-PMHS material. The polysiloxane has a theoretical Si:O ratio of 1:1.025 close to the observed 1:0.85 to 1:0.92 composition. However, the C/Si ratio (0.85 to

0.91) was lower than that expected (0.95) because the fraction of methylhydrogenosiloxane difunctional $SiHCH_3O_{2/2}$ units after sol-gel curing process was decreased, probably due to partial evaporation of cyclic oligomers, as reported previously.[S7,S9]

After the second step, the evolution of chemical composition for the $(R_f)_x(R_{hex})_{1-x}$-PMHS products *versus* the ratio *x*, was listed in Table S3. The final chemical composition resulting of two step-reactions in thin films (sol-gel curing of H-PMHS and hydrosilylation) was compared with the calculated molecular formulae by assuming a fully grafted structure ($\rho = 1$) to the theoretical H-PMHS polymer network summarized as $[Si(R_f)_x(R_{hex})_{1-x}CH_3O_{2/2}]_{0.95}[Si(R_f)_x(R_{hex})_{1-x}O_{3/2}]_{0.05}$. However, such hypotheses are entirely theoretical because in the first step the actual composition of the H-PMHS was not exactly the same as postulated. After the second step, it is found that the matrix have a theoretical Si:O ratio of 1:1.025 in good agreement with the experimental values 1:1.0 to 1:1.025 (Table S3). However, both Si and O atomic compositions compared to those of C and F are in excess from the observed data (Table S3). This suggests that side reaction of SiH groups[S22,S23] of the matrix occurred in competition to hydrosilylation of carbon terminal double bond by diffusion/reaction of alkene moieties.

4. **EDX Spectroscopy**

The surface chemical composition of the functionalized PMHS was further analyzed by EDX as 1–2 µm thick solid films prepared in two steps on silicon wafer (A) or on silicone elastomer Med-4750 (B) sheet (Table S5). For R_{hex}-PMHS on substrate (A), the EDX compositions are very close to values observed from XPS (Table S3). For R_{hex}-PMHS on substrate (B), the silicon content was decreased because the EDX depth of penetration of X-ray was higher compared to the film thickness of about 1 µm. Thus, the overall EDX composition is changed by Med-4750 substrate, whereas this was not expected for the thicker

film (1.9 µm) prepared on substrate (A). In the case of grafted R_f-PMHS film on substrate (B), the fluorine content by EDX (F1s 35.0 atomic %) decreased of 9 % compared to that from XPS value (F1s 44.0 atomic %) also due to the smaller thickness (1 µm) of the R_f-film compared to the EDX probed depth. Despite there is minor variations with XPS results, which are easily explained, we conclude from EDX results that hydrosilylation reaction occurred uniformly in thin film of thickness *ca.* 1 to 2 µm in agreement to FTIR results.

The dotlike patterned surface of R_{hex}-PMHS on silicon wafer A was further characterized by EDX elemental mapping showing that carbon, silicon and oxygen elements are uniformly spread in scanned regions of 25 µm × 50 µm (Figure S17). Thus, the rough and flat areas are identical in term of composition. Moreover, EDX analysis focused on peculiar regions of only 0.25 µm × 0.25 µm, with or without dot formation, also confirmed the chemical homogeneity of different areas (Table S6).

5. Determination of Coefficients of Absorption by Transmission FTIR Measurements

The model used for FTIR calculations is supplied below. The modified Beer-Lambert law can be written as follows: $A_y = \alpha_y h$ where $\alpha_y = F\varepsilon_y C_y$ represents a coefficient of absorption, ε_y and C_y are the characteristic extinction coefficients and molar concentrations associated with a vibration groups *y*, respectively, whereas F is an optical factor at the incidence angle $\theta_i = 0°$ which is related to the refractive indices of substrate and film.[S8] Product $\varepsilon_y C_y$ is characteristic of the material for a specific band because the concentration is fixed by its solid structure. F value is not an important factor in the following analysis. By measuring the absorbance ratio (as peak height *H*), relative to the 2169 cm^{-1} SiH band taken as the external reference, it can be obtained:

$$H_y/H_{2169} = h\varepsilon_y C_y/h_0\varepsilon_{2169}C_0 \quad \text{(S4)}$$

where C_0 = [SiH] is the initial concentration of Si-H groups which also deals with that of the monomer [$OSiHCH_3$] in the pristine H-PMHS film neglecting the silane crosslinker (5% mole) for conciseness. After hydrosilylation, the number of Si-CH_2 bonds formed in the PMHS matrix is the same as that of the Si-H bonds in the starting PMHS matrix assuming a quantitative yield (ρ = 1). The silicon concentrations in H-PMHS and R-PMHS materials for the same sample before and after hydrosilylation are equal and can be written as follows:

$$[\text{Si-H}]_{\text{H-PMHS}} = [\text{Si-CH}_2]_{\text{R-PMHS}} = [(1-x)\text{Si-R}_{\text{hex}} + x\text{Si-R}_{\text{f}})]_{\text{R-PMHS}} \quad \text{(S5)}$$

where R groups are R_{hex} = hexyl and R_f = $C_6F_{13}(CH_2)_3$. The grafting concentration, C_{yi}, of each group *y1* = R_{hex} and *y2* = R_f on silicone chain is given by the following equations:

$$C_{y1} = (1-x)C_o\,[h_0/h]_{\rho=1} \quad \text{(S6)}$$

$$C_{y2} = xC_o\,[h_0/h]_{\rho=1} \quad \text{(S7)}$$

where $[h/h_0]_{\rho=1}$ is the volumetric swelling ratio $(\alpha_f)_{\rho=1}$ of the top gel film in the case of surface-attached film on Si wafer substrate (A) (See also Figure 5a). Thus, Eq. S4 can be simplified by the following Eqs. S8 and S9 for both types of R groups:

$$H_{y1}/H_{2169} = (1-x)\,\varepsilon_{y1}/\varepsilon_{2169} \quad \text{(S8)}$$

$$H_{y2}/H_{2169} = x\varepsilon_{y2}/\varepsilon_{2169} \quad \text{(S9)}$$

The swelling factor does not affect the results if the coating is fully preserved after hydrosilylation as evidenced for all solvents tested because linear correlations were obtained for such a band *versus* molar ratio (*x*) as shown in Figure S5. This also demonstrates clearly that the thickness integrity of the coating is still preserved following hydrosilylation whatever the solvents used. Then, Eq. S8 and Eq. S9 were applied to calculate the normalized coefficients of homogenous polymer $\varepsilon_{CH_2}/\varepsilon_{2169}$ and $\varepsilon_{CF}/\varepsilon_{2169}$ [R-PMHS: R_{hex} (*x* =0) and R_f (*x* = 1)] given in Table S2 from calibration curves in Figure S5 (graph panel top) as follows:

$$y^{CH_2} = x\,(\varepsilon_{CH_2}/\varepsilon_{2169})_{Rf} + (1-x)\,(\varepsilon_{CH_2}/\varepsilon_{2169})_{R_{hex}} \quad \text{(S10)}$$

$$y^{CF} = x\,(\varepsilon_{CF}/\varepsilon_{2169})_{Rf} \quad \text{(S11)}$$

and for calculating the normalized coefficients, $\varepsilon_{SiCH_3}/\varepsilon_{2169}$ and $\varepsilon_{SiOSi}/\varepsilon_{2169}$, from calibration curves given in Figure S5 (graph panel bottom):

$$y^{SiCH_3} = x\,(\varepsilon_{SiCH_3}/\varepsilon_{2169})_{Rf} + (1-x)\,(\varepsilon_{SiCH_3}/\varepsilon_{2169})_{R_{hex}} \quad \text{(S12)}$$

$$y^{SiOSi} = x\,(\varepsilon_{SiOSi}/\varepsilon_{2169})_{Rf} + (1-x)\,(\varepsilon_{SiOSi}/\varepsilon_{2169})_{R_{hex}} \quad \text{(S13)}$$

Other assumptions made for calculations from linear Eqs. S8–S13 were: (*i*) both alkenes have similar reactivity toward hydrosilylation and the ratio of bonds formed by hydrosilylation is the same as that (*x)* of alkenes mixtures, (*ii*) no other bonds are formed or present such as residual SiH, and *(iii)* both alkene reactants have the same ability (size and solubility) to diffuse and react in the slightly crosslinked PMHS material.

6. Measurement of the Surface Energy of R-PMHS Films

To evaluate the dispersive and polar components of the solid surface energy, three liquids were used with the physical characteristics summarized in Table S7. The surface free energy of solid was then calculated by mean of eq. S14 described by Owens and Wendt:[S1]

$$(1+cos\theta)\gamma_L = 2(\gamma_S^d\gamma_L^d)^{1/2} + 2(\gamma_S^p\gamma_L^p)^{1/2} \quad \text{(S14)}$$

$$\gamma_S = \gamma_S^d + \gamma_S^p \quad \text{(S15)}$$

$$\gamma_L = \gamma_L^d + \gamma_L^p \quad \text{(S16)}$$

where θ is the contact angle, γ_S and γ_L are the total surface free energy of the solid and pure liquid, respectively. In these equations, γ_S^d and γ_S^p are the dispersive and polar components of the surface energy of the solid, while γ_L^d and γ_L^p are those of the surface energy of the liquid.

The total surface energy of solid (or liquid) is given by the sum of dispersive (γ^d) and polar (γ^p) components (eqs. S15-S16). Linear relationships are obtained for three solvents (Figure S18), as indicated by fair to good correlation coefficients for R_{hex}-surface ($R^2 = 0.82$) and R_f-surface ($R^2 = 0.999$). The detailed results of calculation are summarized in Table S8.

References

(S1) Owens, D. K.; Wendt, R. C. Estimation of the Surface Free Energy of Polymers. *J. App. Polym. Sci.* **1969**, *13* (8), 1741–1747.

(S2) Johnson, K. L.; Kendall, K.; Roberts, A. D.; Tabor, D. Surface Energy and the Contact of Elastic Solids. *Proceedings of the Royal Society of London. A. Mathematical and Physical Sciences* **1971**, *324* (1558), 301–313.

(S3) Dirany, M.; Dies, L.; Restagno, F.; Léger, L.; Poulard, C.; Miquelard-Garnier, G. Chemical Modification of PDMS Surface without Impacting the Viscoelasticity: Model Systems for a Better Understanding of Elastomer/Elastomer Adhesion and Friction. *Colloids Surf., A* **2015**, *468*, 174–183.

(S4) Ferez, L.; Thami, T.; Akpalo, E.; Flaud, V.; Tauk, L.; Janot, J.-M.; Dejardin, P. Interface of Covalently Bonded Phospholipids with a Phosphorylicholine Head: Characterization, Protein Nonadsorption, and Further Functionalization. *Langmuir* **2011**, *27* (18), 11536–11544.

(S5) Thami, T.; Tauk, L.; Flaud, V. Controlled Structure and Hydrophilic Property of Polymethylhydrosiloxane Thin Films Attached on Silicon Support and Modified with Phosphorylcholine Group. *Thin Solid Films* **2020**, *709*, 138196.

(S6) Nasr, G.; Bestal, H.; Barboiu, M.; Bresson, B.; Thami, T. Functionalization of Polymethylhydrosiloxane Gels with an Allyl Ureido Benzocrown Ether Derivative: Complexation Properties. *J. Appl. Polym. Sci.* **2009**, *111* (6), 2785–2797.

(S7) Thami, T.; Nasr, G.; Bestal, H.; Van der Lee, A.; Bresson, B. Fonctionalization of Surface-Grafted Polymethylhydrosikloxane with Alkyl Side Chains. *J. Polym. Sci. Part A: Polym. Chem.* **2008**, *46*, 3546–3562.

(S8) Bass, M.; Freger, V. Facile Evaluation of Coating Thickness on Membranes Using ATR-FTIR. *J. Membr. Sci.* **2015**, *492*, 348–354.

(S9) Thami, T.; Bresson, B.; Fretigny, C. Tailoring of Elastomeric Grafted Coating via Sol-Gel Chemistry of Crosslinked Polymethylhydrosiloxane. *J. Appl. Polym. Sci.* **2007**, *104* (3), 1504–1516.

(S10) Smith, A. L. *Chemical Analysis, Vol. 112: The Analytical Chemistry of Silicones*; Wiley: New York, 1991; Vol. 112.

(S11) Amro, K.; Clement, S.; Dejardin, P.; Douglas, W. E.; Gerbier, P.; Janot, J.-M.; Thami, T. Supported Thin Flexible Polymethylhydrosiloxane Permeable Films Functionalised with Silole Groups: New Approach for Detection of Nitroaromatics. *J. Mater. Chem.* **2010**, *20* (34), 7100–7103.

(S12) Satoh, Y.; Igarashi, M.; Sato, K.; Shimada, S. Highly Selective Synthesis of Hydrosiloxanes by Au-Catalyzed Dehydrogenative Cross-Coupling Reaction of Silanols with Hydrosilanes. *ACS Catal.* **2017**, *7* (3), 1836–1840.

(S13) Beamson, G.; Briggs, D. *High Resolution XPS of Organic Polymers*; Wiley: Chichester, 1992.

(S14) Alexander, M. R.; Short, R. D.; Jones, F. R.; Michaeli, W.; Blomfield, C. J. A Study of HMDSO/O2 Plasma Deposits Using a High-Sensitivity and -Energy Resolution XPS Instrument: Curve Fitting of the Si 2p Core Level. *Appl. Surf. Sci.* **1999**, *137* (1–4), 179–183.
(S15) Strohmeier, B. R. Evaluation of Polymeric Standard Reference Materials for Monitoring the Performance of X-Ray Photoelectron Spectrometers. *Appl. Surf. Sci.* **1991**, *47* (3), 225–234.
(S16) Gholap, S. G.; Badiger, M. V.; Gopinath, C. S. Molecular Origins of Wettability of Hydrophobic Poly(Vinylidene Fluoride) Microporous Membranes on Poly(Vinyl Alcohol) Adsorption: Surface and Interface Analysis by XPS. *J. Phys. Chem. B* **2005**, *109* (29), 13941–13947.
(S17) Nansé, G.; Papirer, E.; Fioux, P.; Moguet, F.; Tressaud, A. Fluorination of Carbon Blacks: An X-Ray Photoelectron Spectroscopy Study: I. A Literature Review of XPS Studies of Fluorinated Carbons. XPS Investigation of Some Reference Compounds. *Carbon* **1997**, *35* (2), 175–194.
(S18) Hozumi, A.; Takai, O. Effect of Hydrolysis Groups in Fluoro-Alkyl Silanes on Water Repellency of Transparent Two-Layer Hard-Coatings. *Appl. Surf. Sci.* **1996**, *103* (4), 431–441.
(S19) Scofield, J. H. Hartree-Slater Subshell Photoionization Cross-Sections at 1254 and 1487 EV. *J. Electron Spectrosc. Relat. Phenom.* **1976**, *8* (2), 129–137.
(S20) Du, X.; Huang, Z. Advances in Base-Metal-Catalyzed Alkene Hydrosilylation. *ACS Catal.* **2017**, *7* (2), 1227–1243.
(S21) O'Hare, L. A.; Parbhoo, B.; Leadley, S. R. Development of a Methodology for XPS Curve-Fitting of the Si 2p Core Level of Siloxane Materials. *Surf. Interface Anal.* **2004**, *36* (10), 1427–1434.
(S22) Brown-Wensley, K. A. Formation of Si-Si Bonds from Si-H Bonds in the Presence of Hydrosilation Catalysts. *Organometallics* **1987**, *6* (7), 1590–1591.
(S23) Deriabin, K. V.; Lobanovskaia, E. K.; Novikov, A. S.; Islamova, R. M. Platinum-Catalyzed Reactions between Si-H Groups as a New Method for Cross-Linking of Silicones. *Org. Biomol. Chem.* **2019**, *17* (22), 5545–5549.